AD-A032 992 ARMY ENGINEER WATERWAYS EXPERIMENT STATION VICKSBURG MISS F/G 8/7
ENGINEERING PROPERTIES OF CLAY SHALES. REPORT 3. PRELIMINARY TR--ETC(U)
SEP 76 R H PARRY

UNCLASSIFIED WES-TR-S-71-6-3 NL

1 OF 1
AD
A032992

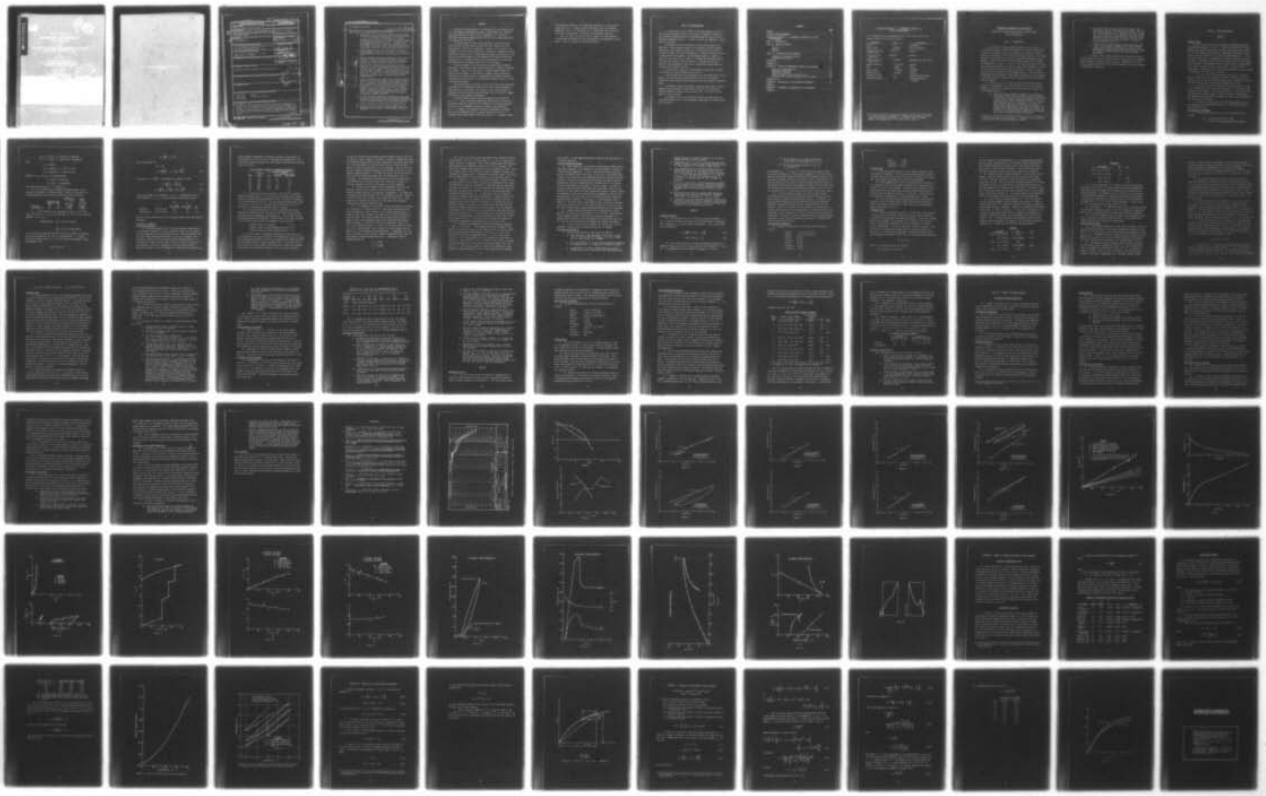

END

DATE
FILMED
1-77

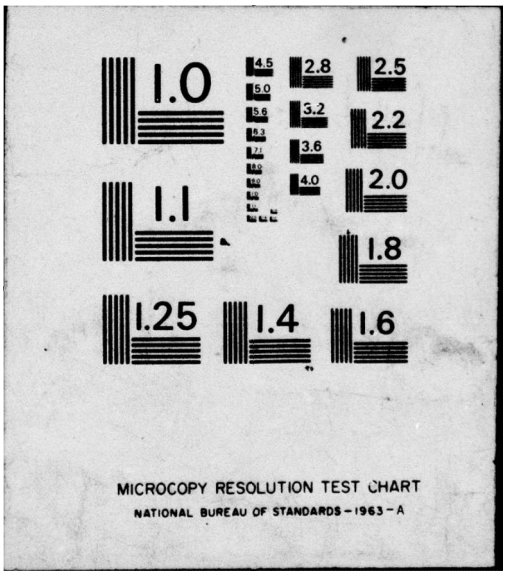
1.0
1.1
1.25
1.4
1.6
1.8
2.0
2.2
2.5
2.8
3.2
3.6
4.0
4.5
5.0
5.6
MICROCOPY RESOLUTION TEST CHART
NATIONAL BUREAU OF STANDARDS - 1963 - A

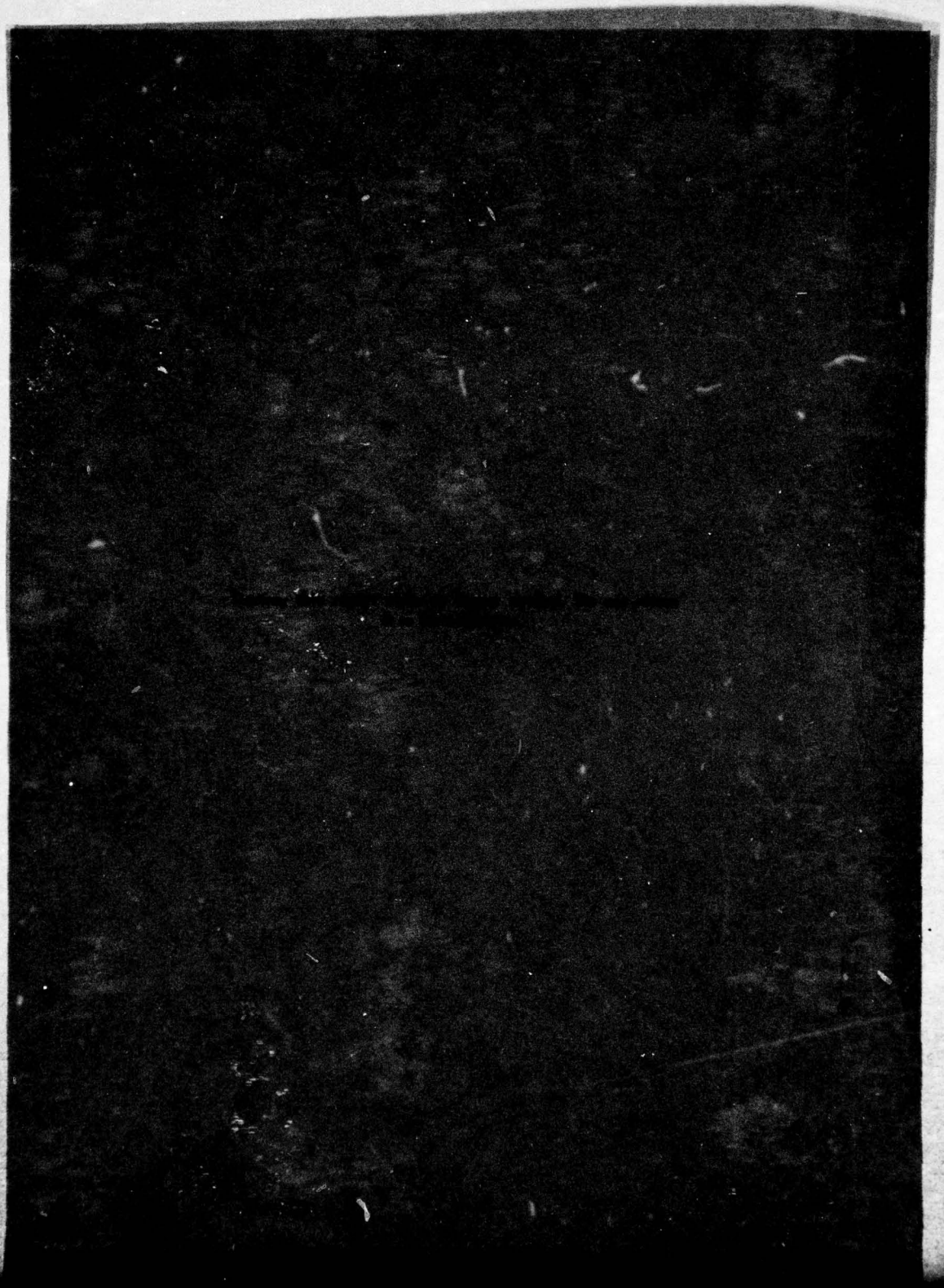

Unclassified

SECURITY CLASSIFICATION OF THIS PAGE (When Data Entered)

(14) WES-TR-S-71-6-3

REPORT DOCUMENTATION PAGE

READ INSTRUCTIONS BEFORE COMPLETING FORM

1. REPORT NUMBER: Technical Report S-71-6, Report 3
2. GOVT ACCESSION NO.:
3. RECIPIENT'S CATALOG NUMBER:

(6) 4. TITLE (and Subtitle): ENGINEERING PROPERTIES OF CLAY SHALES; Report 3, PRELIMINARY TRIAXIAL TEST PROGRAM ON TAYLOR SHALE FROM LANEPORT DAM

5. TYPE OF REPORT & PERIOD COVERED: Report 3 of a series

6. PERFORMING ORG. REPORT NUMBER:

(10) 7. AUTHOR(s): R. H. G. Parry

(9) 8. CONTRACT OR GRANT NUMBER(s): Technical rept.

9. PERFORMING ORGANIZATION NAME AND ADDRESS: U. S. Army Engineer Waterways Experiment Station, Soils and Pavements Laboratory, P. O. Box 631, Vicksburg, Miss. 39180

10. PROGRAM ELEMENT, PROJECT, TASK AREA & WORK UNIT NUMBERS:

(11) Sep 76

11. CONTROLLING OFFICE NAME AND ADDRESS: Office, Chief of Engineers, U. S. Army, Washington, D. C. 20314

12. REPORT DATE: September 1976

13. NUMBER OF PAGES: 82

(12) 81p.

14. MONITORING AGENCY NAME & ADDRESS (if different from Controlling Office):

15. SECURITY CLASS. (of this report): Unclassified

15a. DECLASSIFICATION/DOWNGRADING SCHEDULE:

16. DISTRIBUTION STATEMENT (of this Report)

Approved for public release; distribution unlimited.

17. DISTRIBUTION STATEMENT (of the abstract entered in Block 20, if different from Report)

18. SUPPLEMENTARY NOTES

19. KEY WORDS (Continue on reverse side if necessary and identify by block number)

Clay shales
Laneport Dam
Taylor shale
Shales
Triaxial shear tests

20. ABSTRACT (Continue on reverse side if necessary and identify by block number)

Three triaxial tests were conducted on clay shale specimens from Laneport Dam. The specimens were 3 in. long by 1.4 in. in diameter. The purpose of the test program was to evaluate the influence of temperature variation on pore pressure in clay shale, and stress-strain and pore pressure behavior due to incremental isotropic and axial and lateral stress changes.

(Continued)

Cont. on next p.

DD FORM 1 JAN 73 1473 EDITION OF 1 NOV 65 IS OBSOLETE

Unclassified

SECURITY CLASSIFICATION OF THIS PAGE (When Data Entered)

038100

20. ABSTRACT (Continued).

The results of this experimental program, ~~indicate that for the clay shale studied, the following~~ are given in this report conclusions can be drawn:

a. Temperature rises cause substantial pore pressure increases in clay shale, which increase linearly with effective stress σ' . At $\sigma' = 100$ psi the response is $\Delta u = 6$ psi/°C . The pore pressure changes are not generally reversible and residual pore pressures may be positive or negative, depending on the magnitude of effective stress. At high effective stress they are positive. Some of the temperature effect is due to water in the pore pressure lines and transducer, but this may not be more than a 20 percent effect (Tests T1, T2).

b. Swelling under isotropic stress decrease is linear on a volume change versus log σ' plot, with a $C_s = 0.00887$. On reconsolidation, hysteresis and nonlinearity are observed (T1).

c. The clay shale was found to have anisotropic elastic properties with a lateral stiffness almost twice the vertical stiffness. This has the effect of producing unexpectedly high pore pressures under vertical loads (T1, T2, T3).

d. Under isotropic stress changes, values of pore pressure parameter B were found to range from 0.84 to 0.96, but were usually around 0.90. Under axial stress changes, values of the pore pressure parameter A were found to be up to 0.6 under low axial load, but to decrease gradually under higher axial load. A period of 2 to 4 hr was usually required for the measured pore pressure to stabilize under any stress increment (T2, T3).

e. In the one specimen taken to failure, the deviator stress at failure was 438 psi, which gives a shear strength of almost 16 tsf. A sharp drop in strength occurred after failure, but a stable value of deviator stress of about 270 psi was quickly achieved. The pore pressure change increased progressively to a value of 138 psi at failure and dropped sharply in response to the sharp drop in axial stress after failure. When the postfailure strength reached a stable value, the pore pressure continued to drop slowly but did not approach a negative value (T2).

f. For axial loads up to 20 percent of the failure value, pore pressures and strains were found to be completely reversible, and this was substantially so even for an applied axial stress of 290 psi, equal to 66 percent of the failure value (T2).

g. Failure occurred at an axial strain of 1.2 percent (T2).

h. Inspection of the failed test specimen showed a distinct failure plane with an angle to the horizontal varying from 55 to 63°.

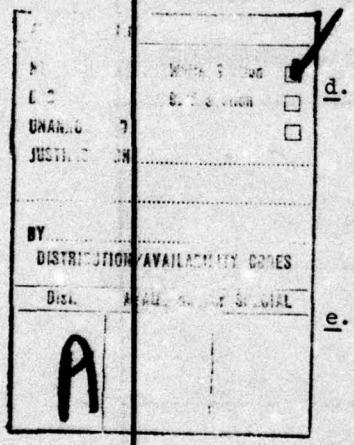

PREFACE

Laboratory investigations of the properties of clay shales by the U. S. Army Engineer Waterways Experiment Station (WES) were requested and authorized by the Office, Chief of Engineers, U. S. Army, in 1965 under Engineering Study (ES) 529 and later in FY 1968 under ES 542 (now designated CWIS 31151).

The initial phase of this study consisted of both laboratory testing by WES and the review of laboratory test results from other laboratories of the Corps of Engineers. Report 1 of this series, "Development of Classification Indexes for Clay Shales," summarizes testing procedures currently used for evaluating the physical properties of clay shales and provided impetus for the adoption of standard pretreatment procedures (i.e., undried, air-dried, and blenderized) for grain-size determinations and Atterberg limits tests on clay shales.

The second phase of the study involved classification indexes, mineralogy, and residual shear strength testing of a number of different clay shales. Report 2 of this series, "Residual Shear Strength and Classification Indexes of Clay Shales," compares various laboratory procedures and equipment used for determining the residual strength of clay shales, and the effects of procedures developed in Report 1 on the classification indexes.

This third phase of the study concerns the concepts and laboratory evaluation of (a) temperature change as it affects the development of pore pressures in clay shale, (b) changes in pore pressure under incremental isotropic and axial stress changes, and (c) effects of sample anisotropy on pore pressure development.

The work conducted under this investigation was performed by Dr. R. H. G. Parry, University Engineering Laboratories, University of Cambridge, Cambridge, England, while serving as a visiting consultant in the Soils and Pavements Laboratory at WES; he was assisted by Mr. R. T. Donaghe, Soils Research Facility, Soil Mechanics Division. The work was conducted under the general supervision of Dr. F. C. Townsend, Chief, Soils Research Facility, and Mr. C. L. McAnear, Chief,

Soil Mechanics Division. The report was prepared by Dr. Parry and reviewed by Mr. S. J. Johnson, Special Assistant, Soils and Pavements Laboratory. Mr. J. P. Sale and Mr. R. G. Ahlvin were Chief and Assistant Chief, respectively, of the Soils and Pavements Laboratory.

COL G. H. Hilt, CE, and COL John L. Cannon, CE, were Directors of WES during the conduct of this investigation and preparation of this report. Mr. F. R. Brown was Technical Director.

AUTHOR'S ACKNOWLEDGEMENTS

I am appreciative of the efforts by Dr. Hoyt Lemons of the U. S. Army European Research Office in London and Mr. Stanley J. Johnson of the Waterways Experiment Station for making possible my visit to the Waterways Experiment Station. It was Mr. Johnson who suggested I should work on clay shale.

All members of the Soils Research Facility group helped me in many ways. Frank Townsend created the environment and Robert Donaghe provided me with constant assistance in conducting tests, not just in a technical sense, but also in helping me to interpret observations and in planning the test program. William Hughes helped in a number of ways, but above all his great skill in trimming test specimens ensured that good test results could be obtained. In mechanical matters Gerald Easley was always at hand and, in particular, helped devise a technique for extension testing.

The smooth way in which the instrumentation worked was a tribute to the efforts of Thomas McEwen and his staff.

I derived great value from discussions on clay shales and on other matters with all the people mentioned above and also with Mosaid Al-Hussaini, Paul Gilbert, and Ed Chisolm of the Soils Research Facility group.

I owe thanks to many other people including Leroy McAnear, Walter Sherman, Joseph Zelasko, M. Juul Hvorslev with whom I had many and varied discussions, James P. Sale, and Don Banks. This work was done under Mr. Sale's purview.

I owe thanks, too, to the library personnel for assisting me in locating references and to the photographic department for making slides for my lectures.

CONTENTS

CONVERSION FACTORS, U. S. CUSTOMARY TO METRIC (SI) UNITS OF MEASUREMENT

U. S. customary units of measurement used in this report can be converted to metric (SI) units as follows:

Multiply	By	To Obtain
inches	25.4	millimetres
cubic inches	16.38706	cubic centimetres
pounds (force) per square inch	6,894.757	pascals
tons (force) per square foot	95,760.52	pascals
pounds (mass) per cubic foot	16.01846	kilograms per cubic metre
degrees (angular)	0.01745329	radians
feet	0.3048	metres
pounds (mass)	0.4535924	kilograms
pounds (force)	4.448222	newtons
inches per minute	25.4	millimetres per minute
Fahrenheit degrees	5/9	Celsius degrees or Kelvins*

* To obtain Celsius (C) temperature readings from Fahrenheit (F) readings, use the following formula: $C = (5/9)(F - 32)$. To obtain Kelvin (K) readings, use: $K = (5/9)(F - 32) + 273.15$.

ENGINEERING PROPERTIES OF CLAY SHALES

PRELIMINARY TRIAXIAL TEST PROGRAM ON TAYLOR SHALE FROM LANEPORT DAM

PART I: INTRODUCTION

1. The triaxial testing program described in this report is of a preliminary nature to define the problems in testing clay shale and to assist in planning a full-scale program on clay shales. Taylor I shale was used because it was the most convenient available. The sample tested was from Laneport Dam, Texas, borehole 8A6C-596, which corresponds to a depth of 54.8-59.2 ft,* the physical properties of which are summarized in Figure 1. In fact, it was found that very good specimens for testing could be cut from the cores of this material. Some of the techniques adopted were makeshift in order to complete a useful program in the few weeks of testing time available. The test results are presented and discussed in some detail, as are some of the problems in triaxial testing of clay shale and an outline of a possible future testing program.

2. Three tests (T1, T2, and T3) were conducted under triaxial conditions on specimens 3 in. (76.2 mm) long by 1.4 in. (35.6 mm) in diameter. The tests are summarized below and described in detail in the following sections.

a. Test T1 was used primarily to measure the influence of temperature change on the development of pore pressures in clay shale. Variations in room temperature were relied on for the work and gave temperature ranges in the test specimen of up to 3°C. The theoretical study of temperature influence requires a knowledge of the amount of swelling and consolidation of the clay shale under isotropic stress change and this property was measured. An attempt to put the specimen under high cell pressure and then fail it in undrained axial compression was abandoned due to water diffusion through the membrane.

---

* A table of factors for converting U. S. customary units of measurement to metric (SI) units is presented on page 5.

b. Test T2 was used to study pore pressure changes under incremental isotropic and axial stress changes. The total axial stress applied in this phase did not exceed 20 percent of the failure stress. Eventually the test specimen was taken to failure in undrained axial compression under strain-controlled conditions, and the test was continued well beyond failure to an axial strain of 4 percent to study postfailure behavior.

c. In Test T3 pore pressure changes were studied under isotropic stress changes, changes in axial stress keeping lateral stress constant and changes in lateral stress keeping axial stress constant, the purpose being to study the effect of specimen anisotropy on pore pressure development.

3. A number of the problems encountered in testing clay shales are discussed in Part III of this report and the outline for a suggested future program of triaxial testing is given. Appendices A, B, and C discuss temperature effects, pore pressure parameters, and the influence of anisotropy, respectively.

PART II: TESTS AND RESULTS

Test T1

Purpose of test

4. This test was set up for the purpose of measuring Skempton's pore pressure parameters A and B^1 under isotropic and axial stress changes, but it was found early in the test that temperature changes of 1 to 2°C were having a marked effect on measured pore pressure values. The most positive evidence for this was the measurement of a B value of greater than unity on increasing the isotropic confining stress by 14.2 psi. This specimen was then used to measure pore pressure changes due to "natural" room temperature rises during the day of approximately 2°C at three different effective stress levels. In one series of measurements, readings were also taken during temperature drop overnight to determine if the effect was reversible.

5. As it was felt that there was some free water in the pore pressure transducers (two transducers were used connected to top and bottom of the test specimen) and connecting lines, a temperature run was also made with the top pore pressure transducer turned off.

6. A theoretical study of temperature effects requires a study of the compressibility and swelling properties of the clay shale under isotropic stress changes. Such a study was made on this specimen, and the opportunity was also taken to assess the degree of anisotropy in the specimen by comparing volume changes with axial length changes under the isotropic stress changes.

7. Finally, the stress-strain and strength characteristics of the specimen were determined by testing it to failure under strain-controlled conditions.

Test specimen information

8. Pertinent characteristics of the test specimen were as follows:

Size: 35.6 mm diam by 76.2 mm long

w: 17.27% from cuttings/16.85% from specimen

e: 0.487 (assuming G = 2.72)/e = 0.478

Saturation: 96.46% initial

Initial setup

9. After trimming a specimen of Taylor clay shale 1.4 in. (35.6 mm) in diameter by 3 in. (76.2 mm) long, it was placed on a triaxial base with 1.4-in.-(35.6-mm)diam by 0.1-in.-(2.54-mm)thick stainless steel porous disks at top and bottom. Two rolled-up membranes were attached to the base pedestal by O-rings. The first membrane was rolled up the specimen to the top cap, then water was allowed into the base of the specimen. This water, together with air trapped between the membrane and specimen, was squeezed out by rolling the second membrane up over the first. If necessary this was repeated. When all visible air was excluded, the second membrane was then rolled up again and both membranes were held against the top cap by O-rings.

10. A spiralled fine-bore (1/16-in.-diam) plastic tube was then attached to the top cap duct to allow drainage or pore pressure measurement. The pore pressure transducer connecting to the top of the specimen was of the differential type in which the back pressure acted on the back of the transducer membrane. The base of the specimen connected to a nondifferential type electrical transducer and to the back pressure/drainage system. The two transducers could be interchanged. Volume change versus pressure characteristics of these transducers was 4×10^{-5} cc/psi .

11. After assembling the cell and introducing the cell water, a pressure of 100 psi was applied to the specimen. An initial pore pressure response of +25 psi was recorded after 48 min standing but this decreased overnight to -2.0 psi. Part of this drop was probably due to a decrease in temperature.

12. Axial load was measured through a 500-lb-capacity load cell. With the assembly used, the axial load could be applied through either load control or strain control. Cell pressure control was through an air pressure regulator and axial deformations were measured with a dial gage having a minimum interval of 0.001 mm. Readings could be interpolated down to 0.0001 mm.

13. The burettes in the drainage/back pressure systems could be read directly to 0.1 cc and interpolated to 0.01 cc. When it was found that temperature was having an important influence on the magnitude of pore pressures, a glass beaker was placed on the triaxial pedestal and partly filled with water into which a thermometer reading directly to $0.1^{\circ}C$ and able to be interpolated to $0.01^{\circ}C$ was immersed.

14. Before starting the testing program a back pressure of 40 psi was applied and the cell pressure was increased to 140 psi. The specimen was left to stand under these stress conditions for a period of three days during which time 0.09 cc of water entered the specimen.

Consolidation-
swelling characteristics

15. When an attempt was made to measure the pore pressure parameter B, a value greater than unity was recorded for an increase in cell pressure of 14.2 psi. This appeared to be due to temperature influence, and observations, described in paragraphs 20-28, were made to determine the pore pressure versus temperature behavior. After some initial temperature runs, the swelling-consolidation characteristics of the specimen under isotropic stress changes were measured and then further temperature runs made.

16. Before starting the swelling-consolidation observations, the specimen was allowed to come to equilibrium overnight under a cell pressure of 160 psi and back pressure of 80 psi. The isotropic effective stress was then decreased to 20 psi by decreasing the cell pressure in increments of 20 psi, allowing 24 hr for equilibrium under each increment. The isotropic effective stress was then increased to 120 psi by increasing the cell pressure to 200 psi in increments of 20 psi, again allowing 24 hr for each increment. The resulting swelling-consolidation plot is shown in Figure 2, as unit volume change Δ_v/v_o in percent versus log effective stress σ' in psi.

17. It can be seen on the semi-log plot of Figure 2 that the swelling line is linear, but the recompression line is distinctly non-linear, so that the material exhibits hysteresis. Values of C_s and C_c in the expressions

$$\Delta e = (1 + e_o)\varepsilon_v = C_s \log \sigma'_o/\sigma' \text{ in swelling}$$
$$\Delta e = (1 + e_o)\varepsilon_{v_o} = C_c \log \sigma'/\sigma'_o \text{ in compression}$$

are:

$$C_s = 0.00887$$

$$C_c = 0.00249 \text{ for } \sigma' = 20 \text{ to } 40 \text{ psi}$$

$$C_c = 0.0258 \text{ for } \sigma' = 80 \text{ to } 120 \text{ psi}$$

Values of m_{vc} and m_{vs} in the expressions

$$\varepsilon_v = m_{vs}\Delta\sigma' \text{ in swelling}$$

$$\varepsilon_v = m_{vc}\Delta\sigma' \text{ in compression}$$

are shown plotted against σ' in Figure 3.

18. It is interesting to compare the volume changes in the specimen with changes in specimen length. These are given below for swelling from 80 to 20 psi and consolidation from 20 to 120 psi:

	Pressure, psi		Change in Unit Volume ε_v, in.^{3}	Axial Strain ε_1, in.
	From	To		
Swelling	80	20	0.00363	0.00193
Consolidation	20	120	0.00555	0.00262

19. If the stiffness of the specimens was equal in all directions, the value of ε_1 should be one-third ε_v, i.e. for an isotropic specimen $\varepsilon_1 = 1/3\ \varepsilon_v$.

Measured ratio $\dfrac{\varepsilon_1}{\varepsilon_v} = 0.536$ in swelling

$$\frac{\varepsilon_1}{\varepsilon_v} = 0.472 \text{ in consolidation}$$

If the vertical and lateral "elastic" moduli with respect to effective stresses are denoted by E'_1 and E'_3, respectively, $n' = E'_3/E'_1$, and Poissons ratio values ν_1, ν_2 are as given in Appendix C, then from Equation C-3a

$$4\Delta\sigma'_1 = \Delta\sigma'_3 = \Delta\sigma'$$

$$\varepsilon_1 = \frac{\Delta\sigma'}{E_1'}(1 - 2\nu_2') \tag{1}$$

and from Equation C-4

$$\Delta\sigma_1' = \Delta\sigma_2'$$

$$\varepsilon_v = \frac{\Delta\sigma'}{E_1'}\left(1 - 4\nu_2' + \frac{2}{n'} - \frac{2\nu_1'}{n'}\right) \tag{2}$$

But putting $\nu_2' = \frac{2\nu_1'}{1 + n'}$ (see Appendix C), Equation 1 gives

$$\varepsilon_1 = \frac{\Delta\sigma'}{E_1'}\left(1 - \frac{4\nu_1'}{1 + n'}\right) \tag{3}$$

$$\varepsilon_v = \frac{\Delta\sigma'}{E_1'}\left(1 - \frac{8\nu_1'}{1 + n'} + \frac{2}{n'} - \frac{2\nu_1'}{n'}\right) \tag{4}$$

Using these equations and assuming $\nu_1' = 0.2$, together with the observed values of ε_1, ε_v for consolidation and swelling, gives

		E_1'	E_3'	
		psi ($\times 10^4$)	psi ($\times 10^4$)	n'
Swelling	80 to 20 psi	2.2	3.8	1.7
Consolidation	20 to 120 psi	2.6	3.8	1.5

Thus the lateral stiffness is 50 to 70 percent greater than the vertical stiffness.

Influence of temperature on pore pressure

20. With the specimen open to both pore pressure transducers or to the bottom transducer only, pore pressure observations were made as the room temperature increased during the day. Some measurements were also made during temperature decrease, in one case overnight, using recorders to obtain a record of pore pressures and temperature. Observations were taken with different isotropic effective stresses in the specimen. The rate of temperature rise was usually between 2 and 4 hr for each 1°C rise in temperature. Measured pore pressures are

plotted against temperature in Figures 4 through 11, and results in pore pressure rise per 1°C rise in temperature are summarized in the following tabulation together with the average effective stress over the range of the test.

Pore Pressure Response to Temperature Changes

Test	σ' (Average) psi	Response, psi/°C		
		Top	Bottom	
			Top Open	Top Closed
T1	64	4.0	4.0	--
T1	93	5.5	5.4	--
T1	94	--	--	5.2
T1	97	--	--	5.5
T1	102	6.5	6.0	--
T1	108	6.3	6.6	--
T2	42	--	--	2.6

21. In Figure 12 the pore pressure rise in psi/°C is plotted against effective stress σ' in psi and it can be seen that a linear increase is shown, passing through the origin. One point in Figure 12 is from observations in Test T2. The pore pressure response rate rises from about 2.4 psi/°C at an isotropic effective stress of 40 psi to 6.0 psi/°C at an isotropic effective stress of 100 psi.

22. It is likely that part of the pore pressure rise during temperature increase is due to the water in the porous stones, ducts, and pore pressure transducers (see Appendix A). The influence of this free water should be in proportion to the volume of free water compared to the volume of water in the soil specimen. The values are:

Volume of water in specimen	24 cc
Volume of water in top transducer and ducts	6 cc
Volume of water in bottom transducer ducts	5 cc

23. In one series of temperature observations (see Figure 10) both transducers were open during the first temperature rise, but during two subsequent temperature rises the top transducer was closed and readings were taken with the bottom transducer only. On the basis of the above figures for water volumes, this should have reduced the observed pore pressure on the bottom transducer by 6/35 or about 17 percent.

In fact, the observed pore pressure response dropped from 6.6 psi/°C to 5.5 psi/°C, a drop of exactly 17 percent. However, a residual pore pressure increase remained after the first temperature run, which meant that in the two subsequent runs the effective stress was lower and this should in itself have resulted in a lower response. The two runs with the top transducer closed are shown by open circles in the plot of pore pressure response versus σ' in Figure 12, and it can be seen that although they lie beneath the drawn line, the difference is only 5 to 10 percent. One observation was made in Test T2 in which there was no top transducer, and its point falls on the drawn line in Figure 12. Thus the influence of water in ducts may be less than expected.

24. Residual pore pressures after a temperature increase, then decrease, such as noted in Figure 10 have been noted before, for example by Henkel and Sowa,[2] as described in Appendix A. The magnitude of residual pore pressure after the first temperature cycle in Figure 10 is about +10 psi, and a further +3 psi after the second cycle. Plum[3] found that it required four cycles for clays before the additional residual pore pressures dropped to zero.

25. It is important to note that for the clay shale, the residual pore pressure is not always positive. Referring to observations with the top transducer, shown in Figure 5, the residual pore pressure is about -2.5 psi, and in Figure 4 the value for the bottom transducer is about -2.0 psi. The reason residual pore pressure may be positive or negative lies in the hysteresis shown by the swelling-consolidation lines in Figure 2. At the end of the first temperature rise in Figure 10, the effective stress σ' is 97.5 psi; at this stress the slope (C_c) of the reconsolidation line in Figure 2 is much steeper than the slope (C_s) of the swelling line (extrapolated). Consequently, the clay shale is stiffer for pore pressure increase (temperature rise) than for pore pressure decrease (temperature drop). Comparative values of compressibility are:

$$C_c = 0.0258$$

$$C_s = 0.00887$$

26. At the end of the first temperature rise in Figure 5, the effective stress is 57 psi; at this stress the C_s and C_c values are almost identical in magnitude. This should probably mean that no hysteresis occurs during temperature cycling, but the plot in Figure 2 was made for very small volume changes and could be slightly in error. There is no doubt, however, that the plot in Figure 2 suggests strongly that residual pore pressures due to temperature cycling are likely to be positive at high effective stress and negative at low effective stress.

27. Using the C_s value for the swelling line in Figure 2, theoretical values of pore pressure increase with temperature rise, using the Plum[3] method, have been presented in Appendix A and the same values are plotted in Figure 12. It can be seen that the predicted values are only about one-half of the observed values at any chosen magnitude of isotropic effective stress σ' . No explanation can be offered for this and it clearly needs further exploration. It seems unlikely that the difference lies in not taking full account of water in the pore pressure lines, porous disks, and transducers, as closing off the top transducer changed the response by an amount very much less than the difference between calculated and observed values. The top transducer system taken out by closing the valve accounted for about half the total free water in lines, etc. It seems unlikely that the true pore pressure response in the specimen (i.e. without any water in lines, etc.) would be less than 5 psi at $\sigma' = 100$ psi from the evidence in Figure 12, whereas the corresponding calculated value is only 2.3 psi/^{o}C.

28. Mitchell and Campanella[4] presented the empirical parameter F where $F = (\Delta u/\Delta t)/\sigma'$. This parameter, which is discussed in Appendix A, usually has a value in the range of 0.007 to 0.013 for clays. For a sandstone porous stone, however, a value of $F = 0.051$ was measured by Mitchell and Campanella[4] with Δt in ^{o}F. Referring to Figure 12 for the experimental line, not corrected for free water in lines, etc., the value of F is $F = 5.9/100 \times 5/9 = 0.033$. Allowing for water in lines, etc., this value would drop to about 0.026. The value of F for clay shale, then, is about midway between the values measured by several workers for clays and the value for the sandstone

porous stone. In this light the measured value for the clay shale is of reasonable magnitude.

Further testing of specimen

29. After completion of the tests to observe pore pressure due to temperature changes, it was intended to test the specimen to failure in undrained axial compression. A test to failure had already been completed on specimen T2 and in the light of this test it was decided that a margin of at least 200 psi was required between cell pressure and back pressure to allow for pore pressure buildup during testing to failure. Consequently, the cell pressure and back pressure were set at 300 and 100 psi, respectively, and allowed to stand for 6 days. In Figure 13 it can be seen that after 6 days water was continuing to flow into the burette at a rate linear with time, suggesting diffusion of water through the membranes or past the O-rings sealing the membranes to the top and bottom platens. At this time, the back pressure valve was closed and the pore pressure observed. The response is plotted against time in Figure 13. The pore pressure rose steadily after closing the back pressure valve, and after 30 hr it had risen from 99 psi to 140.6 psi and was still rising steadily, again indicating diffusion into the specimen.

30. Similar diffusion problems were not encountered in any of Tests T1, T2, and T3 for cell pressures up to 227.5 psi. The problem in T1 was probably related to the high cell pressure and perhaps to a lesser extent to the fact that the specimen had already been under test for a period of 32 days before this higher cell pressure was applied.

31. In view of the diffusion problem, the intention to test the specimen to failure was not pursued and the test was stopped.

Conclusions from Test T1

32. The following conclusions were drawn from Test T1:

a. Under isotropic stress decrements from 80 psi to 20 psi the test specimen swelled linearly on a $\Delta v/v_o$ versus log σ' plot, giving $C_s = 0.00887$.

b. On reconsolidation to 120 psi, hysteresis and nonlinearity were observed with C_c ranging from 0.00249 to 0.0258.

c. A comparison of volumetric changes and axial strains during swelling and consolidation under isotropic stress

changes indicates a lateral stiffness 50 to 70 percent greater than the vertical stiffness.

d. Temperature rises of 2 to 3°C in the specimen gave pore pressure increases varying linearly with effective stress σ', the response at $\sigma' = 100$ psi being 6 psi/°C.

e. Under temperature cycles the pore pressures are not reversible and residual pore pressures may be positive under high values of σ' and negative under low values of σ'. Under one temperature cycle at $\sigma' = 108$ psi a residual $\Delta u = +10$ psi was measured, whereas at $\sigma' = 64$ psi a residual value of $\Delta u = -2.5$ psi was measured.

f. Part of the observed pore pressure-temperature response was due to water in pore pressure lines and transducers but observations with one and two transducers operating indicated this to be not more than 20 percent of the total.

g. The observed pore pressure responses with temperature change were about twice the theoretically calculated values based on the measured C_s and C_c values.

h. An attempt to test the specimen to failure in axial compression was abandoned because diffusion of water through the membranes or sealing rings occurred at the high cell pressure of 300 psi required for the test.

Test T2

Purpose of Test T2

33. This test was set up to obtain pore pressure parameters A and B and to determine the stress-strain characteristics in undrained axial compression. The pore pressure parameters A and B are given in the expression:[1]

$$\Delta u = B\left[\Delta\sigma_3 + A(\Delta\sigma_1 - \Delta\sigma_3)\right] \tag{5a}$$

$$= B\Delta\sigma_3 + BA(\Delta\sigma_1 - \Delta\sigma_3) \tag{5b}$$

34. It is often convenient to study pore pressure change due to deviator stress alone, and for this purpose two new parameters A^+ and A^{++} are introduced and are discussed in Appendix B. In brief:

A^{+} = BA in Equation 5b for total pore pressure change from first application of $(\sigma_1 - \sigma_3)$

A^{++} = BA for any chosen increment of $(\sigma_1 - \sigma_3)$ in undrained test

The parameters B , A^{+} , and A^{++} were first studied under stress-controlled conditions, i.e. by applying increments of isotropic stress or deviator stress under undrained conditions and allowing sufficient time under each increment for the pore pressure to come to equilibrium. During this series, in which three loading-unloading cycles were applied, the deviator stress was not taken beyond 20 percent of the failure value. Pore pressures and strains were completely reversible, this reversibility applying even to a considerable seating effect in the axial strain.

35. A fourth loading-unloading cycle was run under strain-controlled conditions but was stopped and reversed when the load cell was 50 percent overloaded without reaching failure. In addition, the pore pressure reached the cell pressure before this, and subsequent transducer readings were simply the cell pressure and not the pore pressure. Again, on unloading, the pore pressure was completely reversible and the axial strain substantially so, although it showed some hysteresis. After changing the cell and load cell the specimen was finally taken to failure in undrained compression under strain-controlled conditions. After failure, straining was continued to determine post-failure stress-strain behavior.

Test specimen information

36. Pertinent characteristics of the test specimen were as follows:

Height	3.00 in. (76.2 mm)
Diameter	1.394 in. (35.41 mm)
Weight	161.29 g
Initial w	17.01%
Final w	17.14%
Cuttings w	17.20%
Initial e	0.462

Final e	0.466
Cuttings e	0.468
Saturation	96.4%

Initial setup

37. The test specimen was set up in a manner identical to that for the Test T1 specimen. Only one pore pressure transducer (nondifferential type) was used and it was connected to the base of the specimen. Back pressure was applied at the top of the specimen.

38. After assembling the cell and introducing the cell water, a cell pressure of 100 psi was applied, together with a back pressure of 60 psi at the top of the specimen. The specimen was allowed to achieve equilibrium for 4 days under these pressures during which time pore pressures were recorded at the base of the specimen. These pressures were steady at the magnitude of the back pressure after 4 days.

39. Axial load was initially measured through a 500-lb-capacity load cell, but for reading failure under strain-controlled loading a 2000-lb load cell was substituted. Other details of instrumentation were as described for Test T1.

Loading cycle 1

40. After the specimen had stood for 4 days under a cell pressure of 100 psi and back pressure of 60 psi, the back pressure system was closed off and the specimen was ready for testing. In the first loading cycle it was intended to apply axial load increments of 50, 30, and 20 psi, respectively, separated by isotropic increments of 60 and 40 psi, respectively. In order to apply the isotropic increment it was necessary to simultaneously increase the cell pressure and also the piston force to balance additional upward loading on the piston due to the increased cell pressure. This force ΔP is given by the expression:

$$\Delta P = \Delta\sigma_3 \times A_p$$

where $\Delta\sigma_3$ = the increase in cell pressure

A_p = the area of the piston

In fact, however, the multiplication by A_p was inadvertently omitted, with the result that during the two "isotropic" stress increments the axial stress increased by an amount equal to only about two-thirds of the increase in cell pressure, leading to a drop in deviator stress. This drop in stress is shown in the stress path plot in Figure 14.

41. After the fifth loading increment (i.e. third axial load increment), the cell pressure was 200 psi and the axial total stress 265.4 psi. The axial pressure was then decreased in two increments, 50 psi and 15.4 psi. The cell pressure was then decreased in two 50-psi increments to 100 psi, at which point the measured pore pressure was 63.3 psi compared to the pretest value of 63.6 psi. Thus the pore pressure in this load cycle was completely reversible and so was the stress-strain curve shown in Figure 14. The seating effect was not explored in detail in this loading cycle but was noted to be fully reversible.

42. Values of pore pressure parameter A^{++} could be obtained from the three increments of axial loading, and values of B were inferred, using these A^{++} values and observed pore pressure changes in the intended isotropic increments. Equation B-1 (Appendix B) was used to obtain these B values. Values of A^{++} were also calculated for the two axial unloading decrements and the subsequent two decrements of isotropic stress which reduced the cell pressure from 200 to 100 psi. Values of A^{++} for these increments and decrements are given below, together with the estimated B values for the "isotropic" loading increments and B values for the isotropic loading decrements:

	Loading	
Increment	A^{++}	B
$\Delta(\sigma_1 - \sigma_3) = 50$ psi	0.34	--
$\Delta\sigma_3 = 60$ psi	(0.40 assumed)	>0.87
$\Delta(\sigma_1 - \sigma_3) = 30$ psi	0.42	--
$\Delta\sigma_3 = 40$ psi	(0.50 assumed)	>0.88
$\Delta(\sigma_1 - \sigma_3) = 20$ psi	0.67	--

Unloading

Decrement	A^{++}	B
$\Delta(\sigma_1 - \sigma_3) = -50$ psi	0.41	--
$\Delta(\sigma_1 - \sigma_3) = -15.4$ psi	0.49	--
$\Delta\sigma_3 = -50$ psi	--	0.84
$\Delta\sigma_3 = -50$ psi	--	0.97

43. It can be seen that A^{++} values in loading and unloading range from 0.34 to 0.67. The lowest value (0.34) would probably have been higher but the increment was terminated before equilibrium was fully established. The highest value of 0.67 may be too high because of incomplete establishment of equilibrium in the previous increment, as this previous increment was terminated after 1-3/4 hr, whereas the increment with $A^{++} = 0.67$ was maintained overnight. Correct values of A^{++} are probably in the range from 0.4 to 0.6.

44. The values of B range from 0.84 to 0.97, and again the highest and lowest values are suspect as the 0.84 increment was terminated after 2-1/2 hr, whereas the 0.97 increment was maintained overnight.

45. As the pore pressure and axial strain were completely reversible in this first loading-unloading increment, it was decided that further loading cycles should be proceeded with.

Loading cycles 2 and 3

46. In the second loading cycle axial stress increments of 40, 16, 12, and 12 psi were added, in that order, separated by isotropic increments of 40, 30, and 30 psi. After each axial stress increment the ratio $\sigma_1/\sigma_3 = 1.4$. Unloading consisted of removing the axial stress in decrements of 50, 15, and 15 psi, but the isotropic pressure then attained was held at 200 psi and not reduced to the original value of 100 psi.

47. Pore pressure response against time (log scale) is plotted for the various stress increments in Figure 15. It can be seen that there is a gradual rise with time for both A^{++} and B values and usually a period of some 2 to 4 hr is required before equilibrium is reached. This delay is apparently due to the small amount of water

required to flow from the soil specimen to cause the pore pressure to flex the transducer membrane and register the pore pressure. The transducer volume change characteristic is, according to the makers, 4×10^{-5} cc/psi or in terms of specimen strain it is 5×10^{-7} per psi. In Figure 2 the stiffness is of the order of 4×10^{-5} per psi for the soil itself.

48. The third loading-unloading cycle was run using stress-controlled increments to examine the seating strains more closely and to fill in some pore pressure values where the stress increments in the second loading-unloading cycle had been rather large. The third cycle consisted of two small increments of deviator stress, each of 5 psi, followed by further deviator stress increments of 15 and 20 psi, making a total of 45 psi, which was unloaded in two increments, first 15 psi and then 30 psi.

49. Total and effective stress paths on a $(\sigma_1 - \sigma_3)/2$ versus $(\sigma_1 + \sigma_3)/2$ plot are shown in Figure 16b for the second loading-unloading cycle and corresponding pore pressure changes are shown in Figure 17. The stress-strain behavior plotted as $(\sigma_1 - \sigma_3)$ versus axial strain ε_1 for the second and third loading-unloading cycles is shown in Figure 16a and corresponding pore pressure changes for the deviator stress increments only are shown plotted against $(\sigma_1 - \sigma_3)$ in Figure 18a.

50. In the stress-strain plot in Figure 16 it can be seen that between 15- and 20-psi deviator stress is required to establish full seating and the corresponding axial strain is 0.35 percent. Once the seating (which is fully reversible) is established, the stress-strain curve rises steeply and linearly with a total stress elastic modulus E_{ul}, given by Equation C-7 in Appendix C, equal to

$$E_{ul} = 5.4 \times 10^4 \text{ psi}$$

51. The values of A^+ (based on the pore pressure change from start of loading) are shown plotted against $(\sigma_1 - \sigma_3)$ for the second and third loading cycles in Figure 18b. The value drops from 0.5 at $(\sigma_1 - \sigma_3) = 0$ to 0.4 at $(\sigma_1 - \sigma_3) = 80$ psi. These values are remarkably

high for a heavily overconsolidated material, and may be due to anisotropy in the specimen as discussed below.

52. In Figure 19, values of B are plotted against $(\sigma_1 - \sigma_3)$ and these have been taken from the isotropic stress reductions, when $(\sigma_1 - \sigma_3)$ was zero, at the end of the first loading-unloading cycle and from the isotropic stress increments in the second loading-unloading cycle. There is some scatter in these points, but B apparently increases slightly with $(\sigma_1 - \sigma_3)$, from 0.90 to 0.94. If $B = 0.9$, values of the pore pressure parameter A are about 10 percent higher than A^+ and thus A values would be in the range 0.45 to 0.55, based on pore pressures from the start of loading (0.55 is the value at the start of loading).

53. Values of A^{++} for the second and third loading-unloading cycles are also plotted against $(\sigma_1 - \sigma_3)$ in Figure 19. Apart from one rather high value, a reasonably linear plot is obtained in which A^{++} decreases from about 0.51 at the start of loading to 0.26 at $(\sigma_1 - \sigma_3) = 74$ psi. Adopting $B = 0.9$, these A^{++} values represent values of pore pressure parameter A for increments of loading ranging from 0.57 at the start of loading to 0.29 at $(\sigma_1 - \sigma_3) = 74$ psi.

54. In view of the complete reversibility of strain and pore pressure over the loading cycles imposed, the clay shale can be regarded as an elastic material, and it is shown in Appendix C that for an elastic material the pore pressure parameter A depends on the degree of anisotropy. Assuming that Poisson's ratio ν_1' (see Appendix C) is 0.2, and that the elastic moduli with respect to effective stresses vertically and horizontally are E_1' and E_3', respectively, then from Figure C1 in Appendix C:

$$\text{if } E_3' = E_1' \quad A = 0.33$$

$$\text{if } E_3' = 2E_1' \quad A = 0.58$$

$$\text{if } E_3' = 3E_1' \quad A = 0.71$$

55. At the start of application of deviator stress the values of A^+ and A^{++} as measured were 0.5 or slightly higher. Assuming a value of $B = 0.9$ gives

$$A = 0.55 \text{ to } 0.60$$

which suggests that the stiffness of the clay shale in a horizontal direction is about twice that in a vertical direction. Thus, there is little doubt that one of the factors leading to high pore pressure in clay shales in the field is cross-anisotropy with lateral stiffness higher than vertical. The influence of anisotropy on pore pressure is examined further in Test T3.

Loading cycle 4

56. At the conclusion of loading-unloading cycle 3 the test specimen was under an isotropic pressure of 200 psi and the pore pressure was 155.7 psi. The fourth loading cycle was begun by applying a stress increment of 15 psi to overcome seating. The specimen was then loaded at a constant rate of axial compression, initially 0.0000625 in./min, but speeded up to 0.000156 in./min during the test. The test was conducted under undrained conditions.

57. Two unexpected events occurred during the loading cycle:

a. When the deviator stress reached about 100 psi, the pore pressure reached the cell pressure and further increases in pore pressure in the test specimen could not be recorded.

b. When the deviator stress reached 290 psi, the load cell was 50 percent overloaded and further loading was not possible (see Figure 20).

58. When the deviator stress reached the maximum possible with the load cell used, the loading was reversed until the deviator stress reached zero. The pore pressure was again completely reversible, the temperature-corrected value being 155.9 psi compared with 155.7 psi before the start of loading. The axial strain was substantially reversible, the permanent deformation being 0.15 percent compared with the maximum value reached of 1.2 percent. Total stress elastic modulus from the loading curve is consistent between $(\sigma_1 - \sigma_3) = 15$ and 90 psi and again between 150 and 250 psi, the values being

$$(\sigma_1 - \sigma_3) = 15 \text{ psi to } 90 \text{ psi} \qquad E_{ul} = 4.60 \times 10^4 \text{ psi}$$

$(\sigma_1 - \sigma_3)$ = 150 psi to 250 psi $E_{ul} = 3.00 \times 10^4$ psi

Loading cycle 5

59. After completion of the fourth loading-unloading cycle it was necessary to replace the cell surrounding the specimen in order to substitute a load cell of higher (2000-lbf) capacity. This meant that the total stress on the specimen was reduced to zero for about 20 min. When the new cell was fitted the cell pressure was increased to the maximum recordable on the gage, 227.5 psi, and the back pressure was set at 130 psi compared with the pore pressure of 159 psi after the end of the fourth loading-unloading cycle. The test specimen was permitted to achieve equilibrium overnight under this cell pressure and back pressure, and it was hoped that the difference of 97.5 psi would be sufficient to ensure that the pore pressure during shearing would not exceed the cell pressure. In fact, however, this again proved not to be an adequate margin and during subsequent shearing the test had to be stopped temporarily and allowed to partly drain to reduce the pore pressure.

60. After the specimen had reached equilibrium under the cell pressure and back pressure values listed above, the back pressure (drainage) valve was closed and an axial stress increment of 10 psi was added to overcome seating strains. The specimen was then submitted to undrained axial compression at a strain rate of 0.000156 in./min. When $(\sigma_1 - \sigma_3)$ reached 325 psi it was again found that the pore pressure was approaching the cell pressure and the procedure was adopted of stopping the test, holding the axial stress constant by hand, and opening the back pressure valve for 3/4 hr to allow drainage. The valve was then closed and the specimen was allowed 2-1/2 hr to achieve pore pressure equilibrium. The pore pressure drop of 20 psi achieved in this way allowed the specimen to be taken to failure and appeared to have no effect on the specimen behavior.

61. Axial compression was resumed at an increased rate of 0.00031 in./min until failure at $(\sigma_1 - \sigma_3)$ = 438 psi. After failure the strength dropped very rapidly with increasing strain, but it was found that that drop could be followed fairly successfully by turning

off the testing machine and controlling by hand, and in fact for a period putting the machine into reverse. A small pore pressure lag still resulted but this was not of serious magnitude. When the strength reached a stable residual value, constant strain rate was again imposed at the increased rate of 0.00031 in./min until an axial strain of 4.25 percent was achieved.

62. In Figure 21, deviator stress is plotted against axial stress ε_1, together with pore pressure change (corrected for the mid-test adjustment) and A^+. Pore pressure change is plotted against deviator stress in Figure 22 and A^{++} is plotted against deviator stress in Figure 23a. Total stress and effective stress paths are plotted in Figure 23b.

63. Referring to Figure 21, a number of observations may be made as follows:

a. Maximum deviator stress is 438 psi, which is a shear strength of 219 psi or 15.8 tsf.

b. Removing the seating strain, the axial strain at failure is $\varepsilon_1 = 1.2$ percent.

c. The stress-strain curve is linear up to $(\sigma_1 - \sigma_3) = 100$ psi with a modulus $E_{ul} = 7.35 \times 10^4$ psi, and is again linear from $(\sigma_1 - \sigma_3) = 100$ psi to 400 psi with a modulus value $E_{ul} = 4.24 \times 10^4$ psi.

d. A sharp peak occurs at $(\sigma_1 - \sigma_3) = 438$ psi and the strength subsequently plunges very steeply to its ultimate (residual) value of 275 psi. The drop in $(\sigma_1 - \sigma_3)$ from 400 to 300 psi occurs over an axial strain of 0.05 percent.

e. The deviator stress reaches a stable value, dropping only from 275 to 270 psi in the range $\varepsilon_1 = 2$ to 4 percent.

f. The pore pressure change $(u - u_o)$ continues to increase until failure and then drops sharply in response to the drop in deviator stress. This indicates that up to the time the residual strength is reached (at $\varepsilon_1 = 2$ percent) the pore pressure change is wholly governed by stress change. After $\varepsilon_1 = 2$ percent the pore pressure continues to drop gradually although the deviator stress remains almost constant, which suggests that some tendency to structural expansion with shear strain is occurring, but probably only in the immediate vicinity of the failure plane. The dependence of the pore pressure on deviator stress up to and immediately after failure is also reflected in the plot of $(u - u_o)$ versus

$(\sigma_1 - \sigma_3)$ in Figure 22, a sharp drop in pore pressure occurring immediately after failure as the deviator stress drops.

g. The maximum value of pore pressure reached is 132 psi, which corresponds to an A^+ value of 0.3 at failure. However, it can be seen in Figure 21 that in the early stage of loading A^+ is about 0.5, or slightly higher (the values around 0.75 should be ignored as the high-capacity load cell was not calibrated in this low stress range), reducing to 0.3 at failure, then reducing more gradually to 0.2 at the completion of the test with $\varepsilon_1 = 4$ percent.

64. Values of A^{++} shown in Figure 23a are rather scattered in the early part of the test but are around 0.55, dropping almost to zero at failure and then rising again sharply after failure, as the negative pore pressure change due to shear strain starts to assert itself.

Final condition of specimen

65. After reaching $\varepsilon_1 = 4$ percent in the fifth loading-unloading cycle the machine was stopped and it was noted that the deviator stress dropped overnight from 270 to 215 psi due to creep effects and the corresponding pore pressure drop was from 153 to 142 psi. The deviator stress was removed by hand operation of the test machine and then the cell pressure was removed and the cell dismantled. Zero readings on the pore pressure and load cell recorder were checked.

66. Examination of the failed test specimen showed a distinct failure plane, orthogonal views of which are shown in the sketch in Figure 24. The angle of the failure plane varied from about 55 to 63°.

Anisotropy in test specimen

67. Using Equations C-3a and C-10 in Appendix C and Figure C1, values of n' $(= E'_3/E'_1)$, E'_1, and E'_3 can be obtained for load cycles 2 and 3 in Test T2. A value of ν'_1 must be assumed and this is taken as $\nu'_1 = 0.2$. The values of E'_1 and E'_3 are tabulated below, the loading increments adopted being arbitrary and not the same as the actual load increments. The test information was obtained from Figures 16 and 18a.

Values of n', E_1', and E_3' from Loadings 2 and 3

$\sigma_1 - \sigma_3$ Increment psi	Δu psi	B	A	$\Delta\sigma_1'$ psi	$\Delta\sigma_3'$ psi	$\Delta\varepsilon_1$ %	n'	E_1' psi	E_3' psi
0-20	Ignore because of seating								
20-35	6.7	0.92	0.49	8.3	-6.7	0.0003	1.55	3.1×10^4	4.8×10^4
35-50	6.3	0.93	0.45	8.7	-6.3	0.0003	1.40	3.2×10^4	4.5×10^4
50-80	9.5	0.94	0.34	20.5	-9.5	0.0007	1.00	3.2×10^4	3.2×10^4

68. A noticeable feature of these results is that E_1' remains almost constant while E_3' reduces with increasing stress. The values of E_1' of 3.1 to 3.2×10^4 psi agree well with the values of 2.2 and 2.6×10^4 psi measured in Test T1, and the values of E_3' of 3.2 to 4.8×10^4 psi agree with the value of 3.8×10^4 psi measured in Test T1.

Conclusions from Test T2

69. Conclusions drawn from Test T2 are as follows:

a. Increments and decrements of isotropic stress up to 50 psi in magnitude gave values of pore pressure parameter B ranging from 0.84 to 0.96 and averaging about 0.90.

b. Under increments and decrements of axial stress up to 50 psi in magnitude, A^+ values generally ranged from 0.4 to 0.53 and on the average decreased from 0.50 at $(\sigma_1 - \sigma_3) = 0$ to 0.40 at $(\sigma_1 - \sigma_3) = 80$ psi. A^{++} values ranged from 0.25 to 0.59, on the average decreasing from 0.52 at $(\sigma_1 - \sigma_3) = 0$ to 0.25 at $(\sigma_1 - \sigma_3) = 80$ psi.

c. Adopting $B = 0.9$ gives $A = 0.55$ to 0.6 at start of loading, indicating marked anisotropy in the specimen with a lateral stiffness about twice the vertical stiffness, which agrees fairly well with values 50 to 70 percent higher found in Test T1.

d. A period of 2 to 4 hr was required for pore pressures to reach stable values under isotropic and axial stress increments.

e. Under the isotropic and axial stress increments (the total of the latter not exceeding 20 percent of the failure value), pore pressures and strains were found to be completely reversible. This even applied to an observed seating strain.

f. Total stress elastic modulus under axial stress increments was $E_{ul} = 5.4 \times 10^4$ psi.

g. The first attempt to fail the specimen in undrained axial compression under strain-controlled conditions was abandoned because at $(\sigma_1 - \sigma_3) = 290$ psi the load cell was 50 percent overloaded. It was also found that at $(\sigma_1 - \sigma_3) = 100$ psi the pore pressure had risen to the magnitude of the cell pressure and further increases could not be recorded. The pore pressures and strains were again substantially reversible on unloading.

h. After bringing the specimen to equilibrium under a cell pressure of 227.5 psi and back pressure of 130 psi, and substituting a higher capacity load cell, the specimen failed at $(\sigma_1 - \sigma_3) = 438$ psi under strain-controlled undrained compression. This gives a shear strength of 15.8 tsf. Failure strain was 1 to 2 percent.

i. A sharp drop in shear strength occurred immediately after failure, and the specimen reached an ultimate value of $(\sigma_1 - \sigma_3) = 270$ psi.

j. The pore pressure increased progressively up to failure, reaching a value of 132 psi, then dropped sharply in response to the drop in strength. Under continued straining up to 4 percent strain the pore pressure continued to drop gradually.

k. The value of pore pressure parameter A^+ dropped from 0.55 at the start of shear to 0.30 at failure and 0.20 at $\epsilon_1 = 4$ percent.

l. Examination of the failed specimen showed a distinct failure plane with an angle varying from 55 to 63° to the horizontal.

m. The total stress modulus of elasticity in undrained compression E_{ul} is 7.35×10^4 psi up to $(\sigma_1 - \sigma_3) = 100$ psi and 4.24×10^4 psi from 100 to 400 psi from the strain-controlled loading. These were the figures from the second strain-controlled loading (loading cycle 5), the previous cycle having produced lower values of 4.6×10^4 and 3.0×10^4 psi, respectively.

Test T3

Purpose of Test T3

70. This test was set up for the purpose of examining the influence of sample anisotropy on pore pressure by applying different types of stress increments (see Appendix C). The three simple stress

increments adopted were (a) isotropic, (b) changing axial stress while keeping lateral stress constant, and (c) changing lateral stress while keeping axial stress constant. All loadings were under stress-controlled conditions and the test specimen was not tested to failure.

Test specimen information

71. Pertinent characteristics of the test specimen were as follows:

Height	3.00 in. (76.2 mm)
Diameter	1.398 in. (35.5 mm)
Weight	159.53 g (Final 160.42)
Initial w	17.0%
Final w	17.66%
Cuttings w	Not taken
Initial e	0.504 (if G_s = 2.72)
Final e	0.495
Cuttings e	Not taken
Saturation	92%

Initial setup

72. The test specimen was set up in a manner identical to that for the specimen for Test T1. Only one pore pressure transducer was used, connected to the base of the specimen. The back pressure system also connected to the base of the specimen.

73. The top cap was fitted with expandable steel pins, held by an O-ring, which could grip a fitting attached to the piston. This enabled an axial stress of less than the cell pressure to be applied to the specimen. This device was of makeshift design and did not allow strain measurements to be made when testing in the extension mode due to its inherent softness. It could be used, however, for determining pore pressure response.

74. The specimen was permitted to achieve equilibrium under an initial cell pressure of 100 psi and back pressure of 60 psi. Axial load was measured through a 500-lb-capacity load cell, and other instrumentation was as described for Test T1.

Test procedure and results

75. After allowing the test specimen to stand for 4 days under a cell pressure of 100 psi and back pressure of 60 psi, the back pressure valve was closed and isotropic stress was increased in two increments of 20 psi each to obtain values for the pore pressure parameter B . The measured values were 0.81 and 0.83.

76. An attempt was then made to apply a lateral pressure of 30 psi while holding the axial stress constant, but the extension grip device failed to hold and the attempt was abandoned. The cell pressure was then reduced to zero with the specimen sealed against drainage and the cell was dismantled to enable a further O-ring to be fitted around the pins on the gripping device to strengthen the grip. After reassembling the cell, the specimen was allowed to achieve equilibrium overnight under a cell pressure of 120 psi and back pressure of 80 psi. The back pressure valve was then closed and a value of $B = 0.83$ was measured under an increase of 30 psi in cell pressure.

77. An increase of 30 psi in lateral stress was then applied, holding the axial total stress constant, and this was followed by an increase of 30 psi in axial stress, holding the lateral stress constant. This brought the total stress on the specimen to an isotropic value of 180 psi, which was reduced to 150 psi to complete the first loading-unloading cycle.

78. In the second loading-unloading cycle the cell pressure was increased by 30 psi, keeping the axial stress constant, and then the axial stress was increased by 30 psi, keeping the lateral stress constant. The isotropic cell pressure was then increased from 180 to 210 psi. Unloading consisted first of reducing the cell pressure by 30 psi, keeping the axial stress constant, then reducing the axial stress by 30 psi, keeping the cell pressure constant. The isotropic pressure was then reduced from 180 to 150 psi and from 150 to 120 psi. This completed the test.

79. A summary of applied stress increments and pore pressure changes is tabulated on the following page. Immediately prior to the first loading-unloading cycle the test was at equilibrium under a cell

pressure of 120 psi and back pressure of 80 psi. Where necessary, temperature corrections were applied to the pore pressure responses. Values of A in the following tabulation were calculated from the expression:

$$\Delta u = B\left[\Delta\sigma_3 + A(\Delta\sigma_1 - \Delta\sigma_3)\right]$$

adopting a value of $B = 0.90$.

Summary of Pore Pressure Responses

Cycle No.	Applied Stress Change psi	Pore Pressure Change psi	A*	B
1	$\Delta\sigma_1 = \Delta\sigma_2 = \Delta\sigma_3 = +30$	+24.8	--	0.83
1	$\Delta\sigma_1 = 0$, $\Delta\sigma_2 = \Delta\sigma_3 = +30$	+10.9	0.60	--
1	$\Delta\sigma_1 = +30$, $\Delta\sigma_2 = \Delta\sigma_3 = 0$	+15.3	0.57	--
1	$\Delta\sigma_1 = \Delta\sigma_2 = \Delta\sigma_3 = -30$	-27.3	--	0.91
2	$\Delta\sigma_1 = 0$, $\Delta\sigma_2 = \Delta\sigma_3 = +30$	+10.9	0.60	--
2	$\Delta\sigma_1 = +30$, $\Delta\sigma_2 = \Delta\sigma_3 = 0$	+16.2	0.60	--
2	$\Delta\sigma_1 = \Delta\sigma_2 = \Delta\sigma_3 = +30$	+28.0	--	0.93
2	$\Delta\sigma_1 = 0$, $\Delta\sigma_2 = \Delta\sigma_3 = -30$	-11.5	0.57	--
2	$\Delta\sigma_1 = -30$, $\Delta\sigma_2 = \Delta\sigma_3 = 0$	-14.8	0.55	--
2	$\Delta\sigma_1 = \Delta\sigma_2 = \Delta\sigma_3 = -30$	-27.0	--	0.90
2	$\Delta\sigma_1 = \Delta\sigma_2 = \Delta\sigma_3 = -30$	-27.3	--	0.91

* A value of $B = 0.90$ was assumed for calculating A .

80. If the clay shale is elastic and obeys the laws of superposition, then the summation of pore pressure increments for $\Delta\sigma_1 = +30$ psi, $\Delta\sigma_2 = \Delta\sigma_3 = 0$, $\Delta\sigma_2 = \Delta\sigma_3 = +30$ psi should equal the increment for $\Delta\sigma_1 = \Delta\sigma_2 = \Delta\sigma_3 = +30$ psi. In the first cycle the summation gives 26.2 psi, while the isotropic increments give 24.8 psi on loading and 27.3 psi on unloading, so the agreement is reasonable. In the second

cycle the summation on loading gives 27.1 psi compared to 28.0 psi for the isotropic increment, while for unloading the summation is 26.3 psi compared with 27.0 psi and 27.3 psi for the two isotropic unloading decrements. The agreement is again good.

81. In Appendix C it is shown that the pore pressure parameter A is the same for an axial increase in stress and a lateral increase in stress under undrained conditions, even in an anisotropic material. The test results tabulated above strongly support this theoretical prediction.

82. Figure C1 (Appendix C) shows values of A plotted against $n' = E'_3/E'_1$ for values of Poisson's ratio $\nu'_1 = 0.1$ and 0.2 . These plots came from the theoretical expressions in Equation C-13. Values of A equal to 0.55 to 0.60 observed in Test T3 correspond theoretically to values of n' of 1.7 to 2.1 for $\nu'_1 = 0.2$ and 2.2 to 2.6 for $\nu'_1 = 0.1$. Values of n' from Tests T1 and T3 are as follows:

n' Values from Tests T1 and T3

	Test T1		Test T3	
	$\nu'_1 = 0.2$	$\nu'_1 = 0.1$	$\nu'_1 = 0.2$	$\nu'_1 = 0.1$
Swelling	1.75	2.0	1.7 to 2.1	2.2 to 2.6
Consolidation	1.5	1.6		

Conclusions from Test T3

83. Conclusions drawn from Test T3 were as follows:

a. Under isotropic stress increments and decrements, the value of pore pressure parameter B ranged from 0.90 to 0.93 with one exception of B = 0.83 for the first increment.

b. Under increments and decrements of axial stress equal to 30 psi, the pore pressure change ranged from 14.8 to 16.2 psi, giving an average value of pore pressure parameter A = 0.57 (assuming B = 0.90).

c. Under increments and decrements of lateral stress equal to 30 psi, keeping axial stress constant, the pore pressure change ranged from 10.9 to 11.5 psi, giving an average value of A = 0.59 .

d. The above observations are consistent with an elastic material having a lateral stiffness of about twice the vertical stiffness.

PART III: FUTURE CLAY SHALE RESEARCH

Problems in Testing Clay Shale

84. A number of problems arise in testing clay shales which may be less significant in testing other softer and less brittle materials. Some of these problems are discussed below.

Calibration of equipment

85. In view of its high stiffness, the deformation of clay shale under working load is small and in order to record these movements accurately careful calibration is required. For example, dial gage movements should be recorded with a very rigid dummy specimen for changes in cell pressure. Similarly, dial gage movements arising from temperature changes in the cell assembly should be both measured and calculated.

86. The present burettes used in the back pressure system are not sensitive enough for small specimens of clay shale and replacement of these should be considered.

Temperature effects

87. Temperature effects have a marked effect on recorded pore pressure, although it is uncertain at this time how much of this is due to the test specimen and how much to water in the pore pressure lines and transducers. It is suggested later* that a study should be made of temperature effects, but for all other testing the test specimens and testing equipment should be kept at a temperature constant within $\pm 0.1^{\circ}C$. Calibration of temperature effects alone is not an answer to this problem as pore pressure changes arising from cyclic temperature changes are not reversible.

88. If possible, the whole testing room should be maintained at $\pm 0.1^{\circ}C$, but if this is not possible it will be necessary to enclose and isolate each test system to maintain it within this temperature tolerance.

---

* Under "Suggested Future Work."

Seating effects

89. It was observed in Test T2 that under initial small axial stress increases the axial compression was relatively large, even though the specimen had been under isotropic pressure of 200 psi and effective stress of 100 psi. The stiffness increased suddenly when the axial deformation was about 0.2 mm, corresponding to an axial strain of 0.3 percent and deviator stress of 15 psi. This seating proved to be reversible and may be due to one or all of the following:

a. Seating of piston into top cap.

b. Seating of porous disks against top and bottom platens.

c. Seating of porous disks against top and bottom of test specimen.

The most likely cause is a as b and c are both under as much as 100-psi effective stress before axial loading, so the additional 15 psi to cause seating is relatively very small to have such an effect.

90. It is likely that the piston-top cap contact slips slightly on application of a small load, pushing the piston slightly off alignment to establish a firm contact. This would be reversible as observed. Notwithstanding this belief, the origin of the seating should be investigated further because any seating effects due to the specimen to porous disk contacts could materially affect studies related to anisotropy of clay shale. If there is any porous disk to sample seating effect, it may be necessary to put a smear of cement on the ends of the specimen before seating it, but this cement would need to be sufficiently porous not to impede movement of water into or out of the specimen.

Need for high cell pressure

91. In testing clay shale specimens to failure, high pore pressures can be induced because of the very large stresses required to cause failure. In order that these pore pressures can be recorded it is necessary to establish an adequate margin between the initial back pressure and the cell pressure at which the test is to be conducted. The back pressure should be at least 60 psi and in some cases perhaps a little higher as the pore pressure rise recorded in Test T2 up to

failure was 138 psi. Allowing a 50 percent margin on this gives a difference between cell pressure and back pressure of 210 psi and thus a cell pressure of at least 270 psi and possibly higher is required.

92. At present, the bleed control regulators which are necessary for this work have a maximum capacity of 200 psi, so higher capacity regulators will be needed. If nitrogen cylinders are used for pressure supply these may drain quickly with bleed control regulators and will have to be watched carefully.

93. At the high pressure difference of 210 psi or so, the possibility of water diffusion through the membrane arises. After the final temperature tests had been completed in Test T1, the test specimen was set at a cell pressure of 300 psi and back pressure of 100 psi for a period of 6 days. In Figure 13 it can be seen that water was continuing to flow into the burette after 6 days at a rate which was linear with time. This suggests diffusion either through the membranes or past the O-rings sealing the membranes to the top and bottom platens. At this time, the back pressure valve was closed and the pore pressure observed. The pore pressure was still rising after 30 hr, again indicating diffusion of water into the test specimen.

94. This problem can probably be solved either by using three of the present membranes with silicone grease coating between each or two thicker membranes, and by the use of three O-rings at top and bottom somewhat tighter than the present O-rings. Leakage problems were not encountered in any of the test specimens for cell pressures up to 227.5 psi.

Brittleness of test specimen

95. In Test T2 the strength dropped very sharply after failure. This poses the problem of following the stress-strain curve in this phase and also of recording pore pressures accurately if the load drops sharply.

96. In trying to control the test immediately after failure it is necessary that the loading system be very hard so that there is very little stored energy to be imparted to the specimen as it fails. In fact, the 2000-lb-capacity load cell used for Test T2 probably deforms

about 0.002 in. over its full load range so that the system is fairly hard. But even a system of this hardness may not be adequate and a servocontrol system might be necessary, particularly as there can, with some materials, actually be some strain recovery during the rapid load drop after failure. A servocontrol machine would be expensive and it may be sufficient to provide such control by hand--this was done with some success in Test T2 and with experience even greater success could be achieved. It may be necessary even to reverse the machine as part of this control.

Modification for extension testing

97. In studying the effects of anisotropy it is essential that different stress paths can be applied. A simple and useful variation on applying an axial compressive load, keeping cell pressure constant, is to be able to increase the cell pressure, keeping the axial stress constant. This requires a positive locking of the piston to the top cap of the test specimen so that the cap can be pulled against the cell pressure, which enables an axial stress less than the cell pressure to be achieved.

98. In Test T3 a very simple clutching device was used to achieve this effect, but it is not suitable as a permanent technique because:

a. It has a low load capacity.

b. It deforms appreciably under load.

c. There is a large movement of the piston between applying upward and downward loads on the top cap.

99. In cells where the piston can be turned a threaded or bayonet type locking system can be devised, but in this case, with the use of rolling diaphragms, the piston cannot be turned. The most probable method of solving the problem will be to bore a hole down the middle of the piston into which a rod can be inserted capable of locking together the piston and the top cap.

Suggested Future Work

Samples

100. The preliminary triaxial testing to date has been confined

to Taylor clay shale from Laneport Dam. It has proved to be a particularly amenable material to work with and further testing should be done on it, but preferably on fresh samples as the cores used for this program have been in storage for some 2 yr. Tests should also be performed on a minimum of one of two other shales which exhibit high pore pressure in field loading, such as the Dawson shale at the Chatfield dam site and the Pepper shale at Waco Dam. Tests should also be performed on one or more shales in which high pore pressures do not develop in the field.

101. It is strongly recommended that fresh clay shale samples be obtained, transported, and stored under the supervision of a member of the WES Soils Research Facility group.

Temperature effects

102. It has been shown in the preliminary program that in the laboratory quite small temperature changes can cause marked changes in pore pressure in clay shale test specimens. This has important implications on:

a. The laboratory testing of clay shales.

b. Methods of sealing, transporting, and storing clay shale specimens.

c. Behavior of clay shales in the field at near-surface levels where temperature changes can occur.

103. It is clear that laboratory tests on clay shales should normally be performed in an environment where the temperature variations are not greater than 0.1°C. However, temperature effects in themselves are important and should be made a study in their own right, particularly since the values measured in the Taylor clay shale exceed theoretical values. Future temperature studies should be made over strictly controlled temperature cycles, rather than relying on fluctuations in room temperature as in the preliminary program. Temperature changes should be gradual, perhaps 1°C every 2 hr, and all parts of the test equipment including pore pressure lines and transducers, as well as the test specimen, should be at the same temperature.

104. One point not resolved in the testing to date is the

contribution of water in pore pressure lines and transducers to temperature-pore pressure changes, although it appears that this may have been of the order of a 20 percent contribution in Test T1. The effect is lessened as the volume of water in the test specimen increases with respect to the volume of water in the ducts, etc., and for this reason it is suggested that corresponding studies should be made on 3-in.-long by 1.4-in.-diam specimens and on two larger sizes, say 6-in.-long by 2.8-in.-diam and 8-in.-long by 4-in.-diam.

105. The development of residual pore pressures under cyclic stress changes should be studied, particularly in relation to confining stress and stress history. It appears that the residual pore pressures may be positive or negative depending on stress history and perhaps on temperature history.

106. Some thought should be given to methods of sealing, transporting, and storing clay shale cores, as appreciable temperature rises could bring about sharp pore pressure increases which, allied with zero confining pressure, could expose weakness in the clay shale structure and cause its breakdown. Pouring hot wax around a core to seal it would seem to be a particularly destructive technique.

Anisotropy in clay shale

107. It has been shown in this report that Taylor clay shale is strongly anisotropic and that this anisotropy can have a marked influence on pore pressure development under load. To a large extent it may be anisotropy which distinguishes a clay shale which develops large pore pressures in the field under loading from one which does not. Clearly, then, these studies should be extended, perhaps as follows:

a. Submission of triaxial test specimens to different applied stress paths to study pore pressure development under undrained conditions as in Test T3.

b. Submission of triaxial test specimens to different applied stress paths to study volume changes under drained conditions.

c. Submission of test specimens to isotropic stresses under drained conditions to study volume changes and relative axial and radial strains.

Where volume changes are to be measured, specimens not smaller than 6 in. long by 2.8 in. in diameter should be used so that an appreciable volume change will be measured. The volume change characteristics over swelling and consolidation cycles will also be required for the temperature studies as in Test T1.

108. Useful information may also be obtained by testing specimens cut at different inclinations with respect to relative moduli in different directions and with respect to the effect of anisotropy on shear strength.

Specimens with preformed weaknesses

109. Clay shales in the field will not be uniform homogeneous materials, but will contain various weaknesses--some local, some extensive. These may be in the form of fissures, joints, bedding features, horizon interfaces, etc., which may not normally be open but in fact have an appreciable strength, but markedly lower than that of the basic clay shale matrix.

110. It has been shown in the work described in this report that the basic clay shale can develop high positive pore pressures, particularly if it is anisotropic, for stresses less than failure. In the field, failure will occur long before the shear stress reaches the shear strength of the basic clay shale, so that when failure develops along weaknesses, high positive pore pressures will be present in the basic blocks of clay shale. Movement along the weaknesses may tend to produce negative pore pressures in their vicinity (this is uncertain), but these will be swamped out by the positive pore pressures in the basic material. Only minute migrations of water would be required in these stiff materials to achieve this effect. It is the combination of weaknesses plus positive pore pressure which has probably produced some of the unexpected behavior of clay shales in the field.

111. It should be possible to study the above-mentioned type of behavior in laboratory specimens by:

a. Precutting failure planes in triaxial specimens at, say, angles of 15°, 30°, 45°, and 60° to the horizontal (one plane per specimen) and inserting a pore pressure probe into the plane or into a slightly undersized

prebored hole close to the plane. Measurement of pore pressures by the probe and also at the ends of the specimen could indicate if the above-suggested mechanism might be possible in the field.

b. Failing a specimen and stopping the test as soon as it reaches a reasonably stable strength following failure, then inserting a pore pressure probe into the failure zone, in such a direction that the probe would not be damaged by further straining. The specimen could then be retested and taken to a substantial axial strain, observing the probe pore pressures and those at the ends of the specimen. It is likely that the intact portions of the specimen will again develop positive pore pressures on retesting even though the specimen has been failed.

Cyclic loading

112. In view of the high positive pore pressures which develop in undrained axial compression it is possible that cyclic loading could produce a progressive buildup in pore pressures. These could find their way into weak zones and produce instability in a clay shale mass. Thus, in relation to earthquake studies and blast effects, it could be revealing to perform laboratory tests with slow cyclic loading and pulse loading on triaxial specimens with and without preformed weaknesses to study pore pressure effects.

REFERENCES

1. Skempton, A. W., "The Pore-Pressure Coefficients A and B," Geotechnique, Vol 4, No. 4, 1954, pp 143-147.

2. Henkel, D. J. and Sowa, V. A., A discussion of "Creep Studies on Saturated Clays," Laboratory Shear Testing of Soils, Special Technical Publication No. 361, Dec 1964, pp 104-110, American Society for Testing and Materials, Philadelphia, Pa.

3. Plum, R. L., The Effect of Temperature on Soil Compressibility and Pore Pressure, M.S. Dissertation, Cornell University, Ithaca, N. Y., 1968.

4. Campanella, R. G. and Mitchell, J. K., "Influence of Temperature Variations on Soil Behavior," Journal, Soil Mechanics and Foundations Division, American Society of Civil Engineers, Vol 94, SM3, May 1968, pp 709-734.

5. Ladd, C. C., Physico-Chemical Analysis of the Shear Strength of Saturated Clays, Sc. D. Dissertation, Massachusetts Institute of Technology, Cambridge, Mass., 1961.

6. Mitchell, J. K. and Campanella, R. G., "Creep Studies on Saturated Clays," Laboratory Shear Testing of Soils, Special Technical Publication No. 361, Dec 1964, pp 90-103, American Society for Testing and Materials, Philadelphia, Pa.

7. Atkinson, J. H., The Deformation of Undisturbed London Clay, Ph. D. Dissertation, University of London, London, England, 1973.

8. Gibson, R. E., "The Analytical Method in Soil Mechanics," Geotechnique, Vol 24, No. 2, 1974, pp 115-139.

9. Harr, M. E., Foundations of Theoretical Soil Mechanics, McGraw-Hill, New York, 1966.

10. Henkel, D. J., "The Relevance of Laboratory Parameters in Field Studies," Proceedings, Roscoe Memorial Symposium, 1971, pp 669-675.

11. Pickering, D. J., "Anisotropic Elastic Parameters for Soil," Geotechnique, Vol 20, No. 3, 1970, pp 271-276.

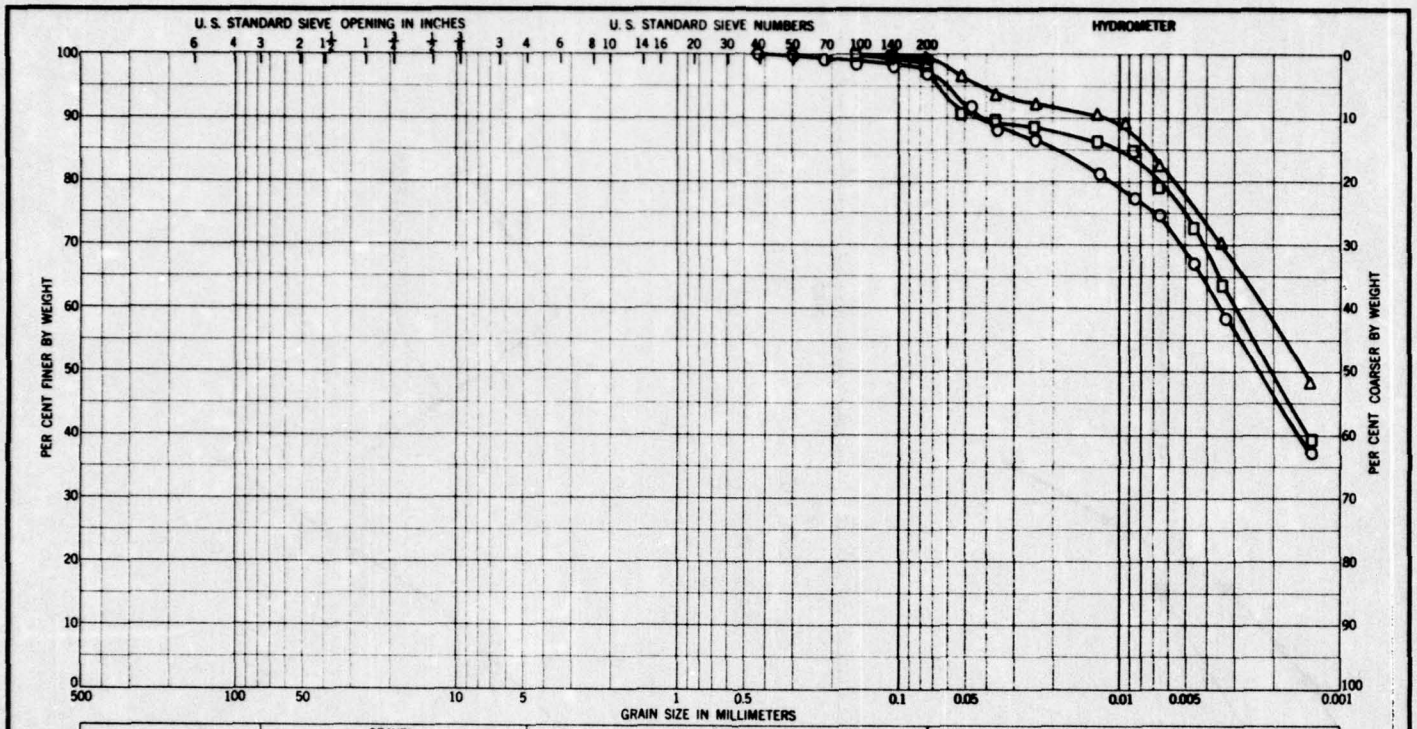

Sample No.	Elev or Depth	Classification	Nat w %	LL	PL	PI
UNDRIED	○	CLAY (CH) WITH TRACES OF		65	22	43
AIR-DRIED	□	FINE SAND		65	21	44
BLENDERIZED	△	(GRAY)		79	21	58
		2.70 G_S (EST)				
		W_{NAT} = 18.4 - 19.1 %				

GRADATION CURVES

Project	TAYLOR I SHALE
	DEPTH 60.7-61.7 FT
Area	LANEPORT DAM
Boring No.	8A6C-596
Date	12 OCTOBER 1970

WES FORM NO. 1241
SEPT. 1962

Figure 1. Physical properties of Taylor I shale, Laneport Dam

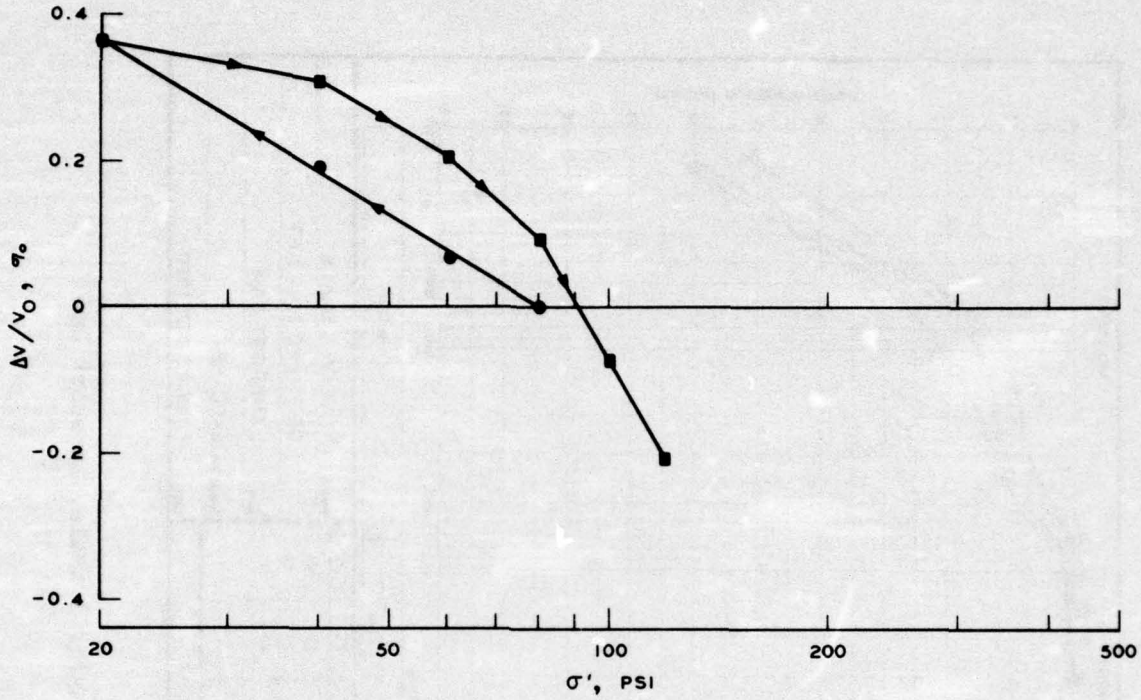

Figure 2

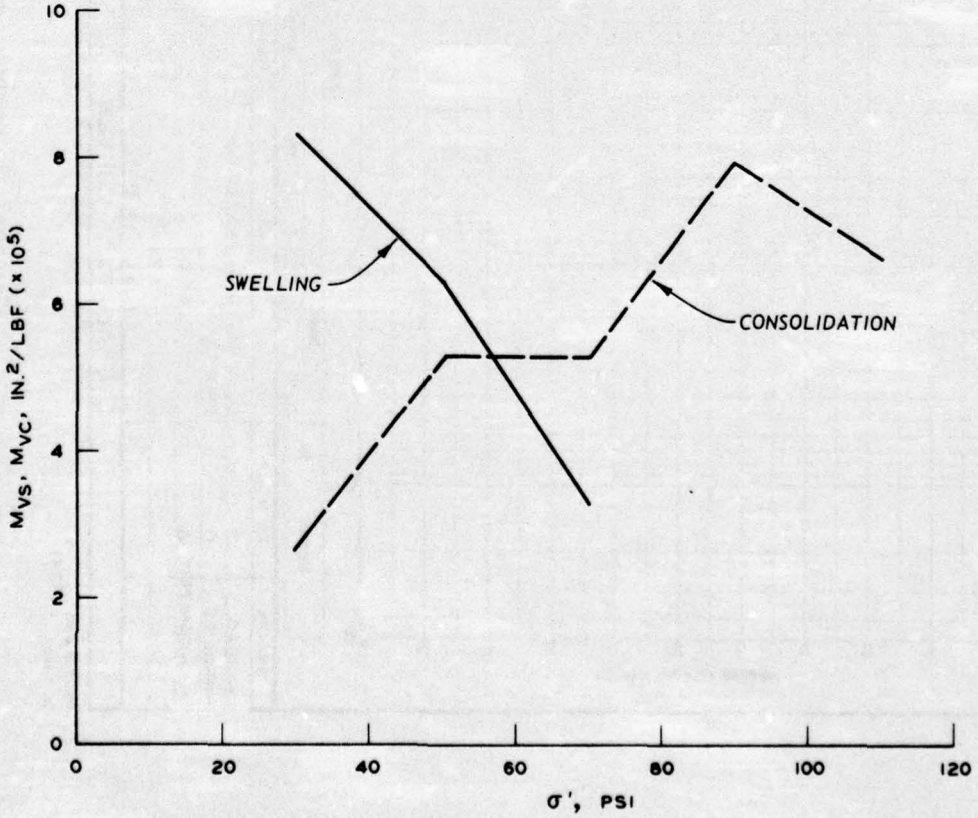

Figure 3

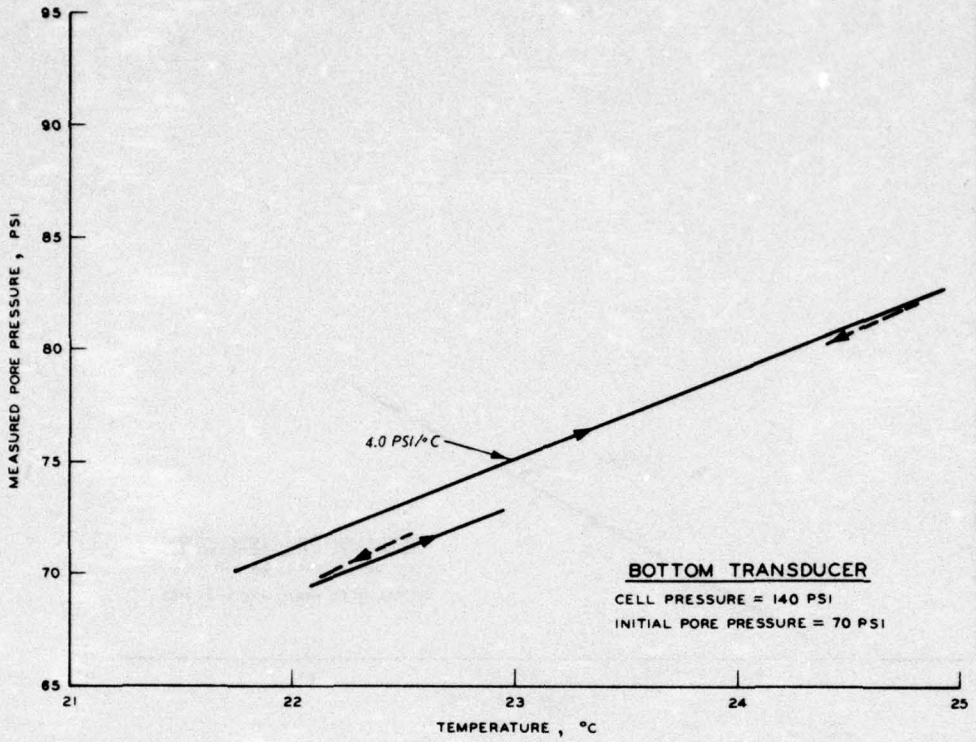

Figure 4

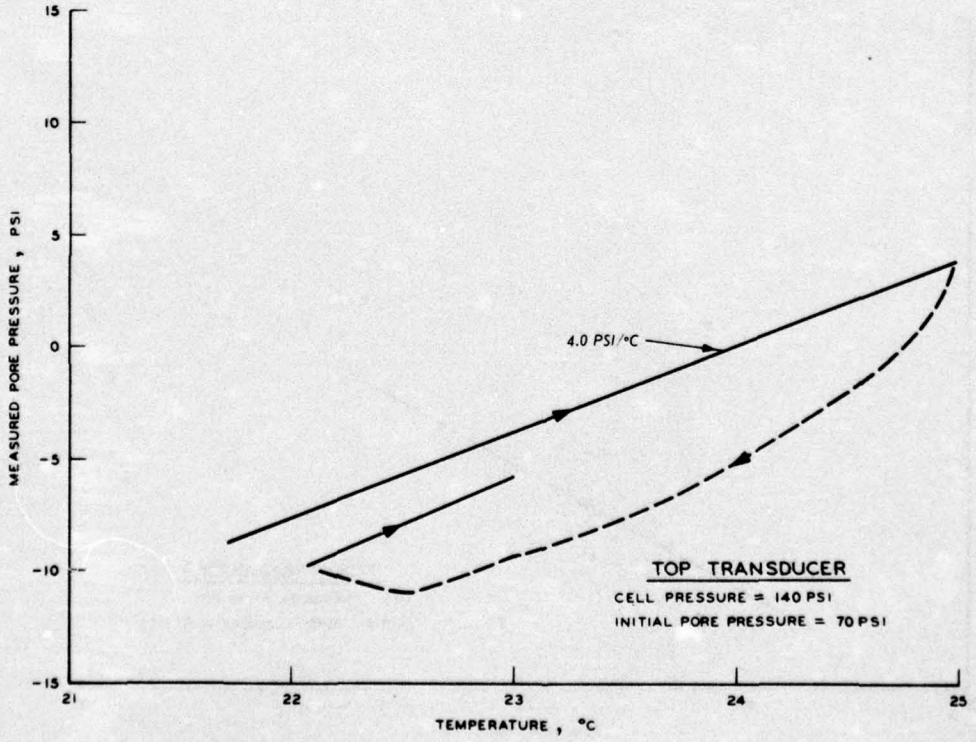

Figure 5

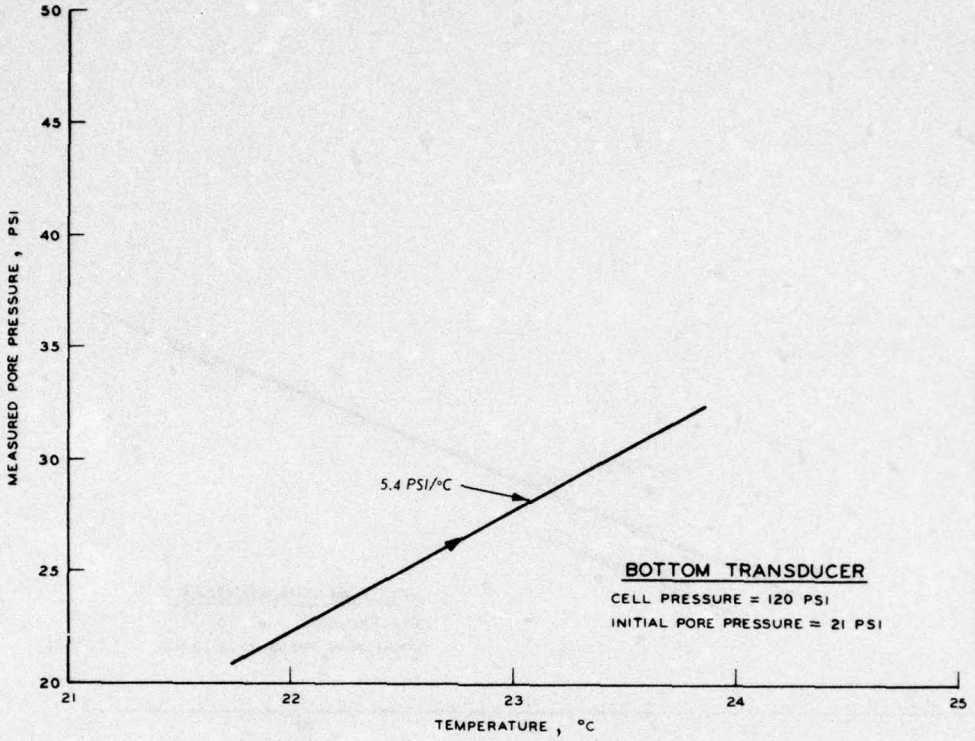

Figure 6

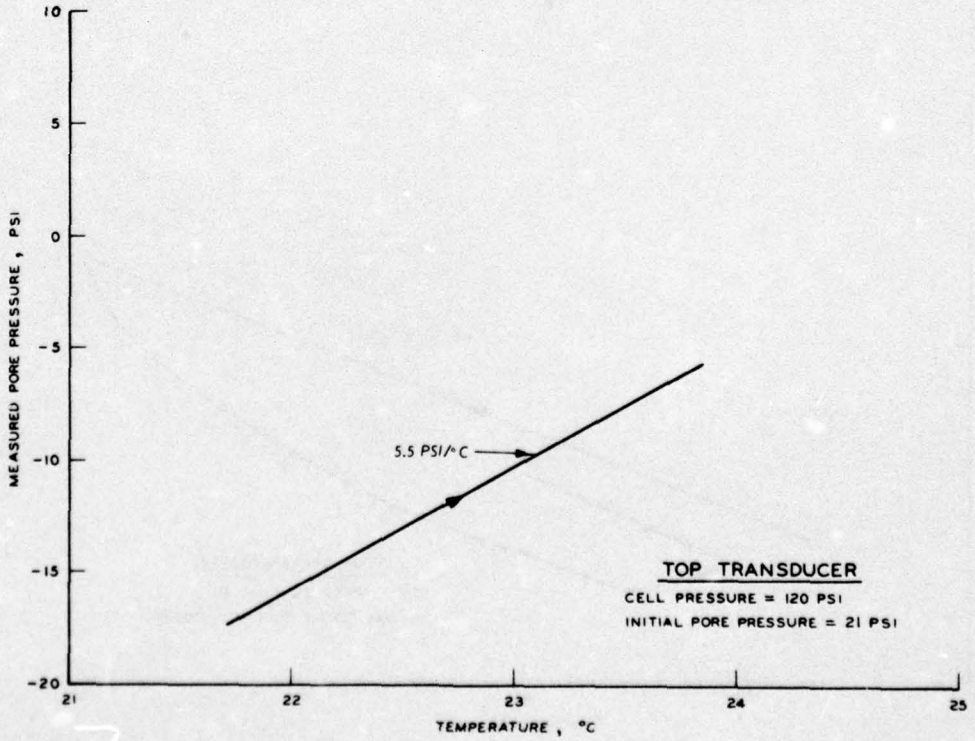

Figure 7

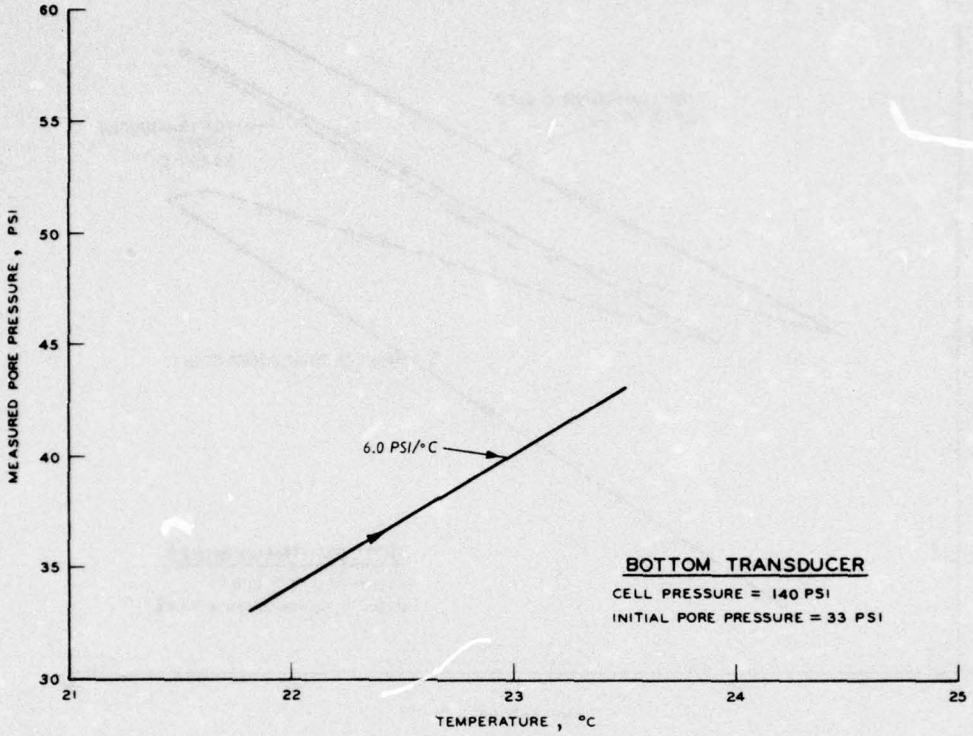

Figure 8

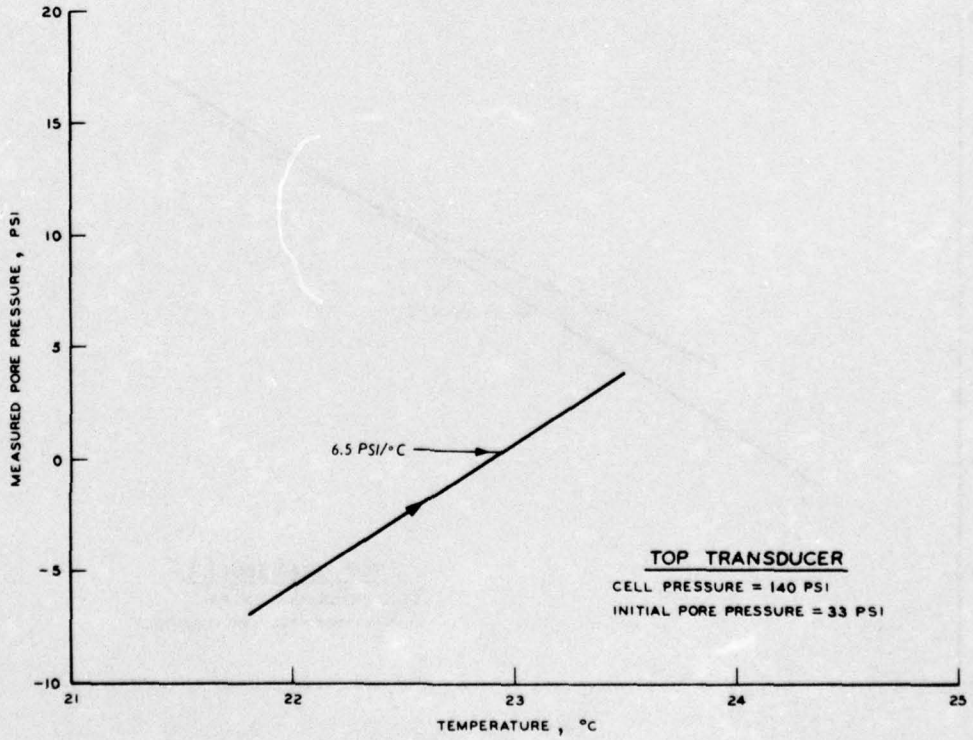

Figure 9

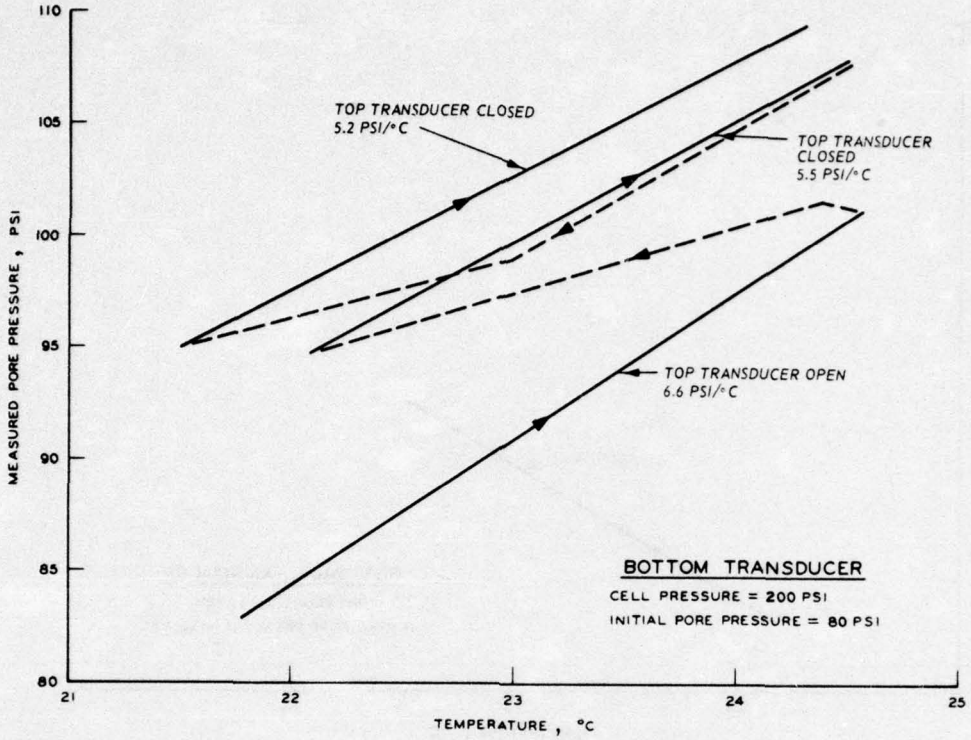

Figure 10

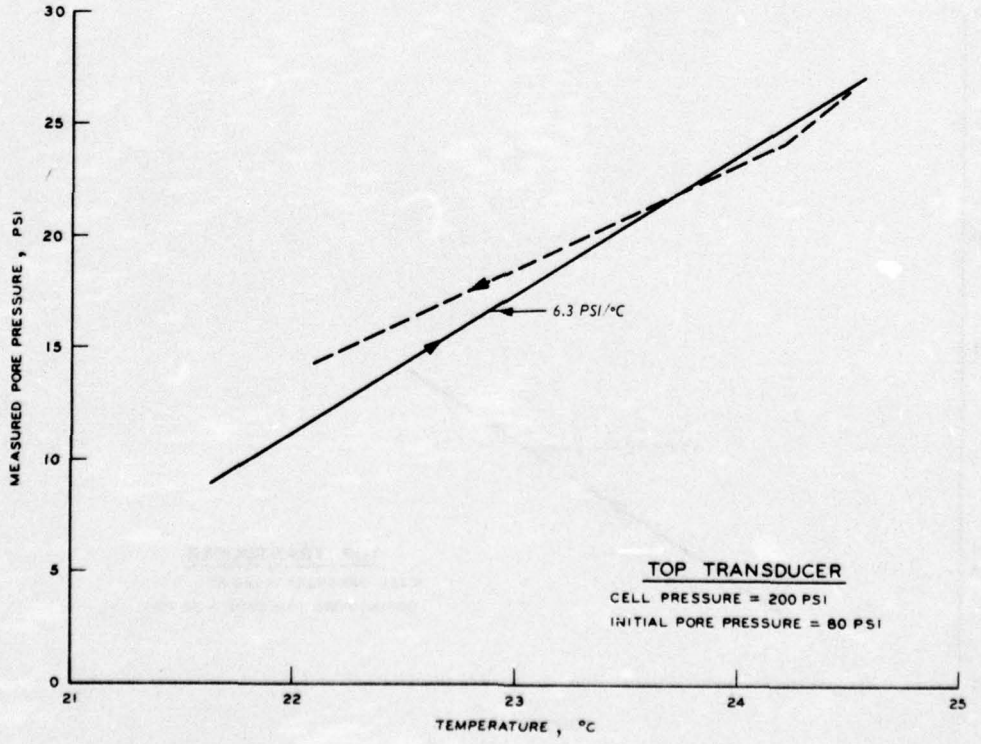

Figure 11

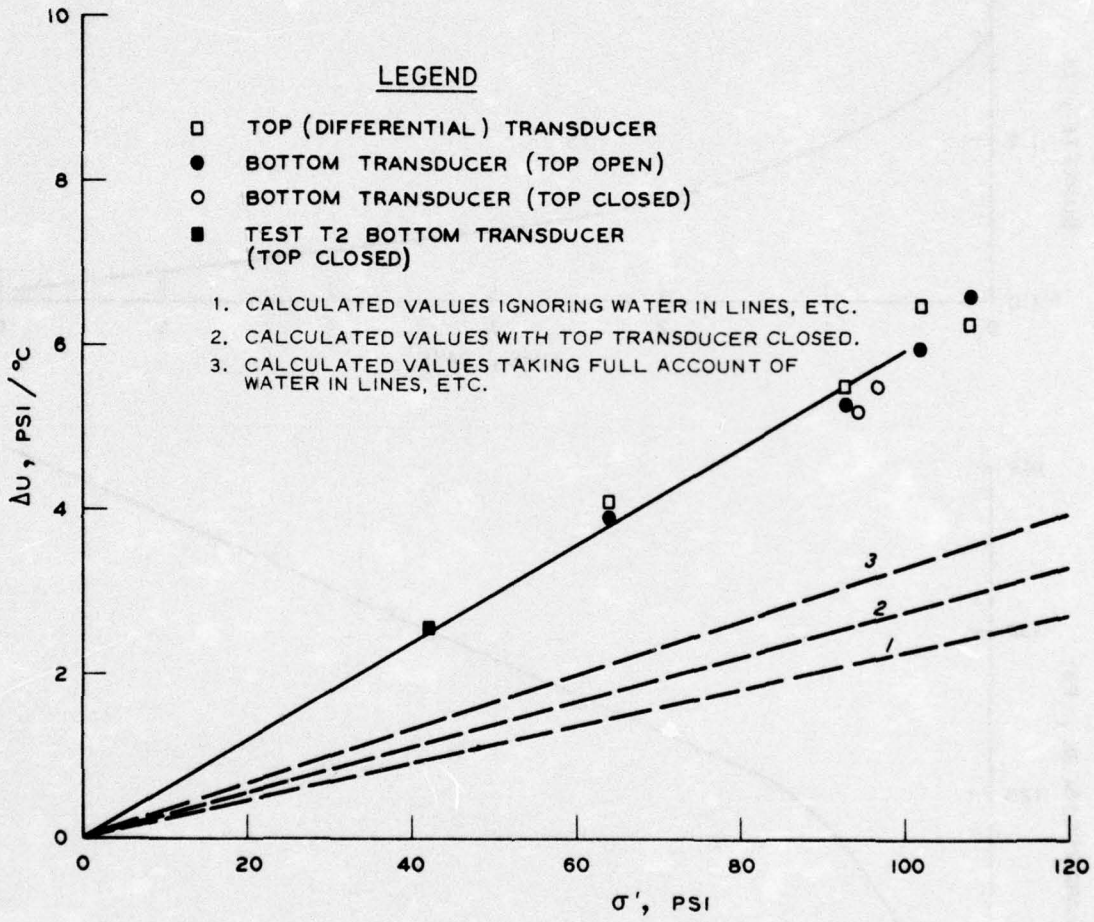
LEGEND
TOP (DIFFERENTIAL) TRANSDUCER
BOTTOM TRANSDUCER (TOP OPEN)
BOTTOM TRANSDUCER (TOP CLOSED)
TEST T2 BOTTOM TRANSDUCER (TOP CLOSED)
1. CALCULATED VALUES IGNORING WATER IN LINES, ETC.
2. CALCULATED VALUES WITH TOP TRANSDUCER CLOSED.
3. CALCULATED VALUES TAKING FULL ACCOUNT OF WATER IN LINES, ETC.
Δu, PSI / °C
σ', PSI
0
2
4
6
8
10
0
20
40
60
80
100
120
1
2
3

Figure 12

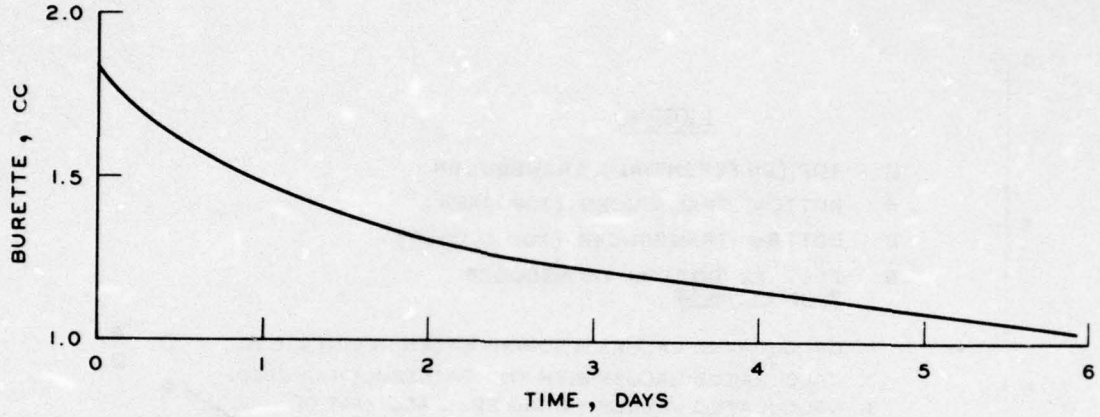
2.0
1.5
1.0
BURETTE , CC
0
1
2
3
4
5
6
TIME , DAYS

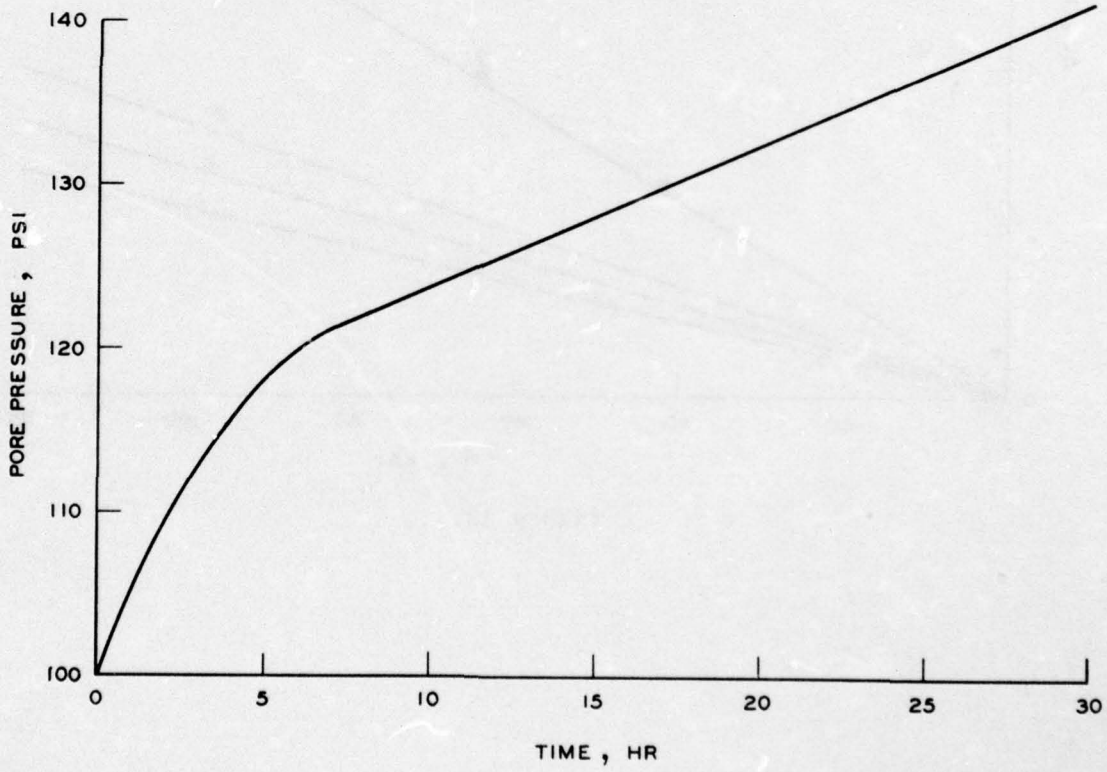
140
130
120
110
100
PORE PRESSURE , PSI
0
5
10
15
20
25
30
TIME , HR

Figure 13

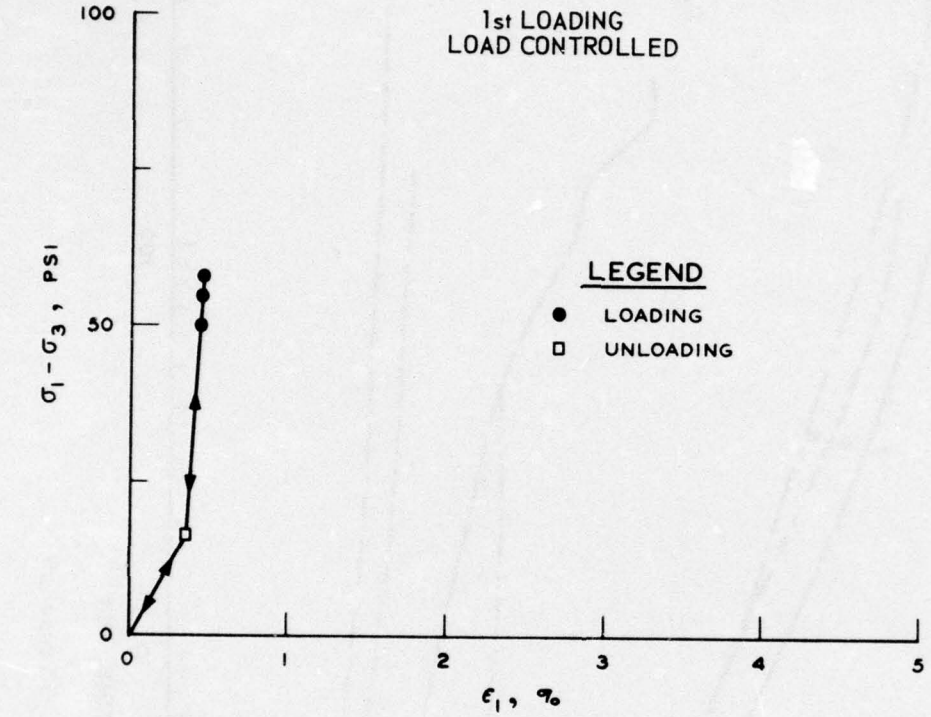
1st LOADING
LOAD CONTROLLED
LEGEND
LOADING
UNLOADING
100
50
0
$\sigma_1 - \sigma_3$, PSI
0
1
2
3
4
5
ϵ_1, %

a.

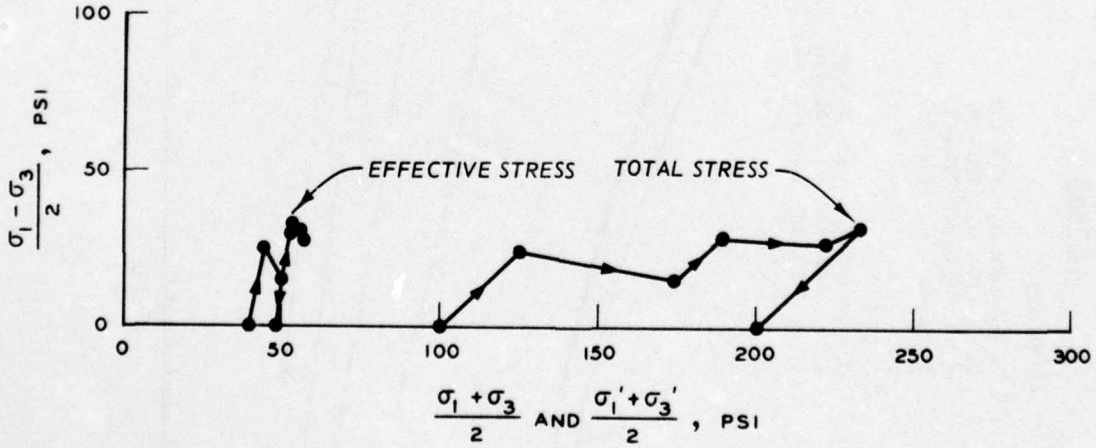
100
50
0
$\frac{\sigma_1 - \sigma_3}{2}$, PSI
EFFECTIVE STRESS
TOTAL STRESS
0
50
100
150
200
250
300
$\frac{\sigma_1 + \sigma_3}{2}$ AND $\frac{\sigma_1' + \sigma_3'}{2}$, PSI

b.

Figure 14

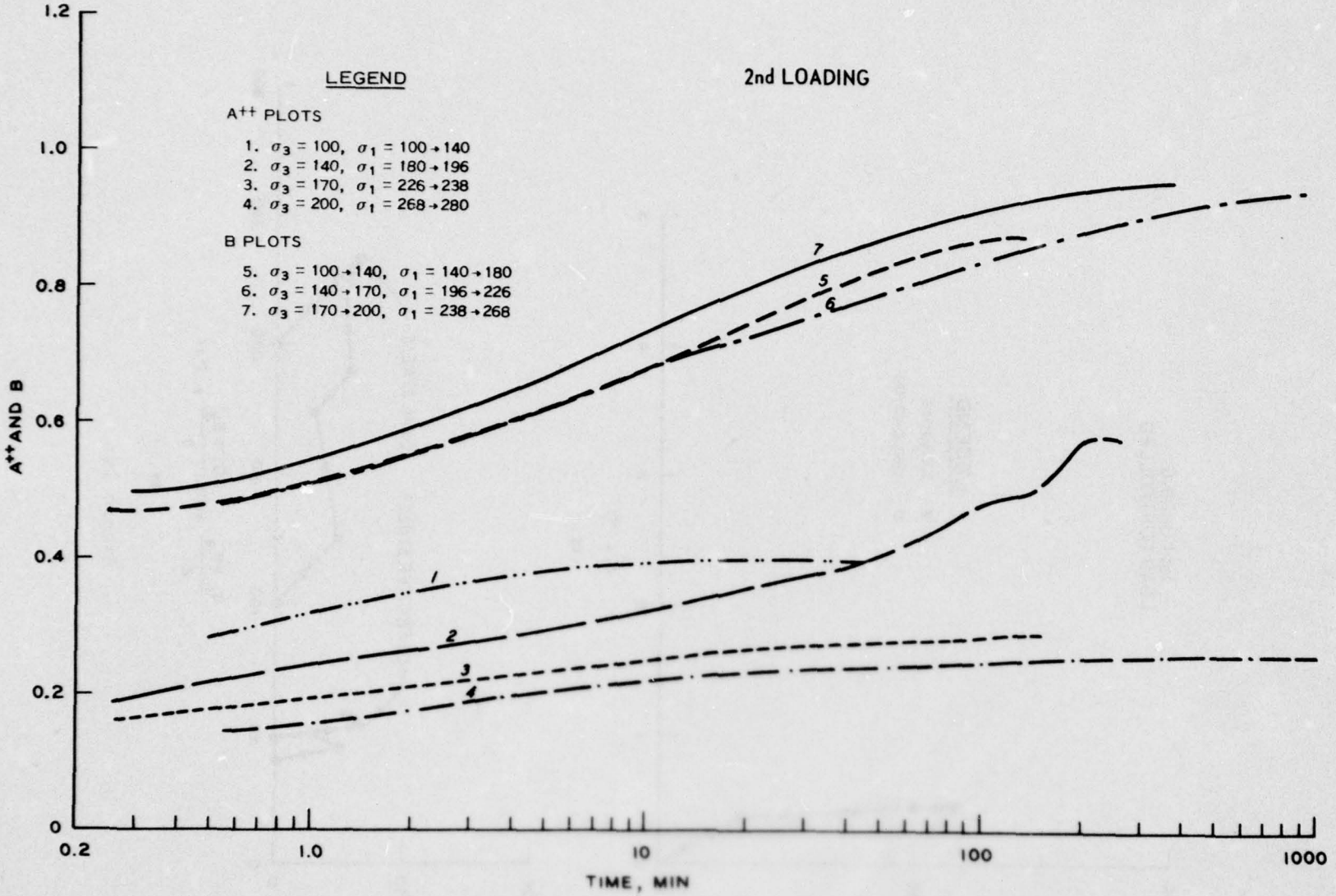
LEGEND
A++ PLOTS
1. σ3 = 100, σ1 = 100→140
2. σ3 = 140, σ1 = 180→196
3. σ3 = 170, σ1 = 226→238
4. σ3 = 200, σ1 = 268→280
B PLOTS
5. σ3 = 100→140, σ1 = 140→180
6. σ3 = 140→170, σ1 = 196→226
7. σ3 = 170→200, σ1 = 238→268
2nd LOADING
A++ AND B
TIME, MIN
0
0.2
0.4
0.6
0.8
1.0
1.2
0.2
1.0
10
100
1000

Figure 15

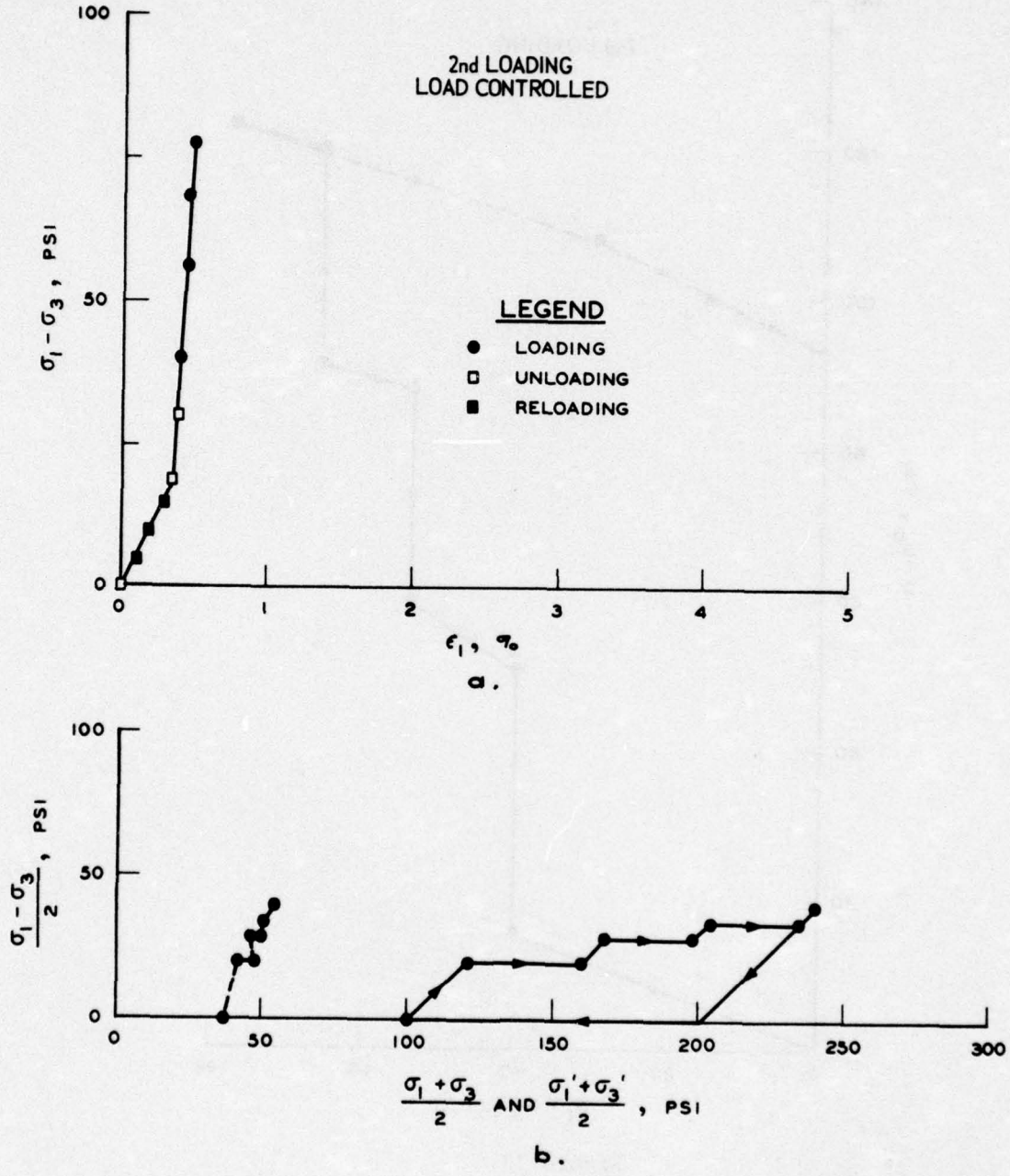
2nd LOADING
LOAD CONTROLLED
LEGEND
LOADING
UNLOADING
RELOADING
100
50
0
$\sigma_1 - \sigma_3$, PSI
0
1
2
3
4
5
ϵ_1, %
a.
100
50
0
$\frac{\sigma_1 - \sigma_3}{2}$, PSI
0
50
100
150
200
250
300
$\frac{\sigma_1 + \sigma_3}{2}$ AND $\frac{\sigma_1' + \sigma_3'}{2}$, PSI
b.

Figure 16

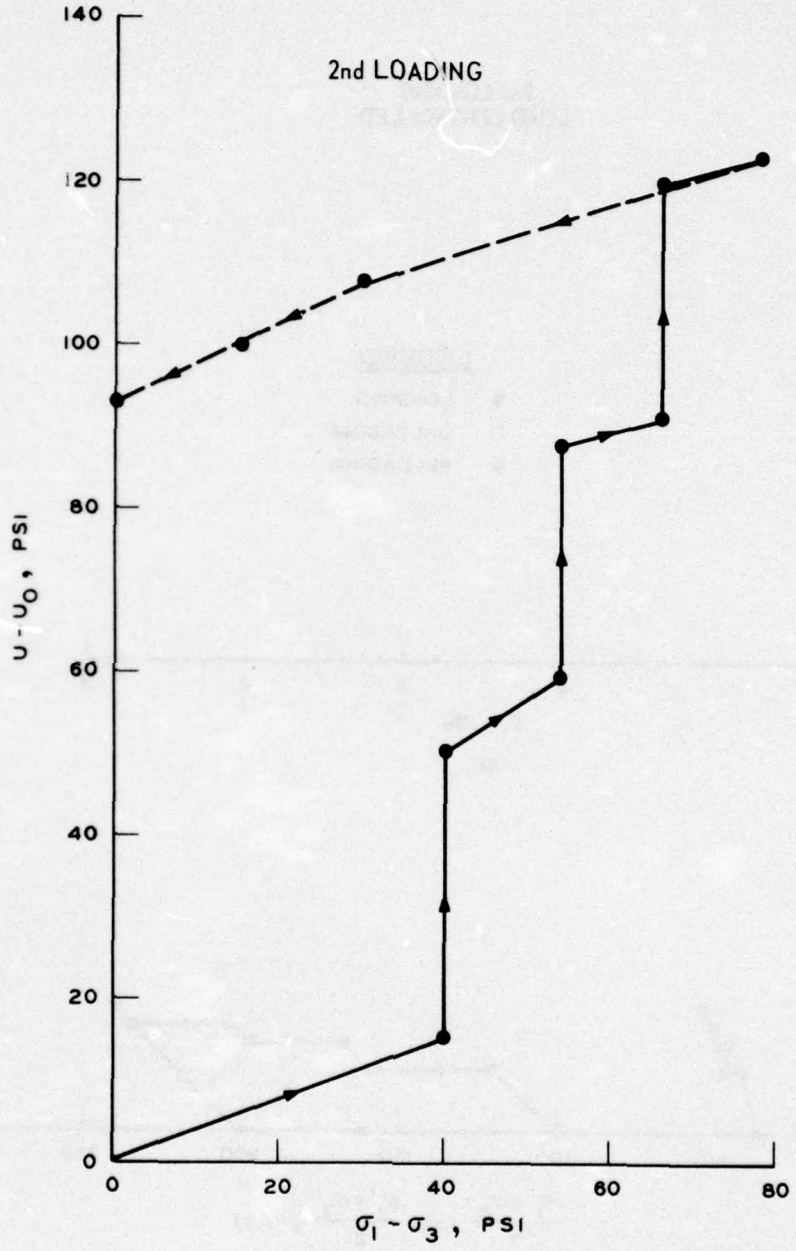
2nd LOADING
140
120
100
80
60
40
20
0
U - U0 , PSI
0
20
40
60
80
σ1 - σ3 , PSI

Figure 17

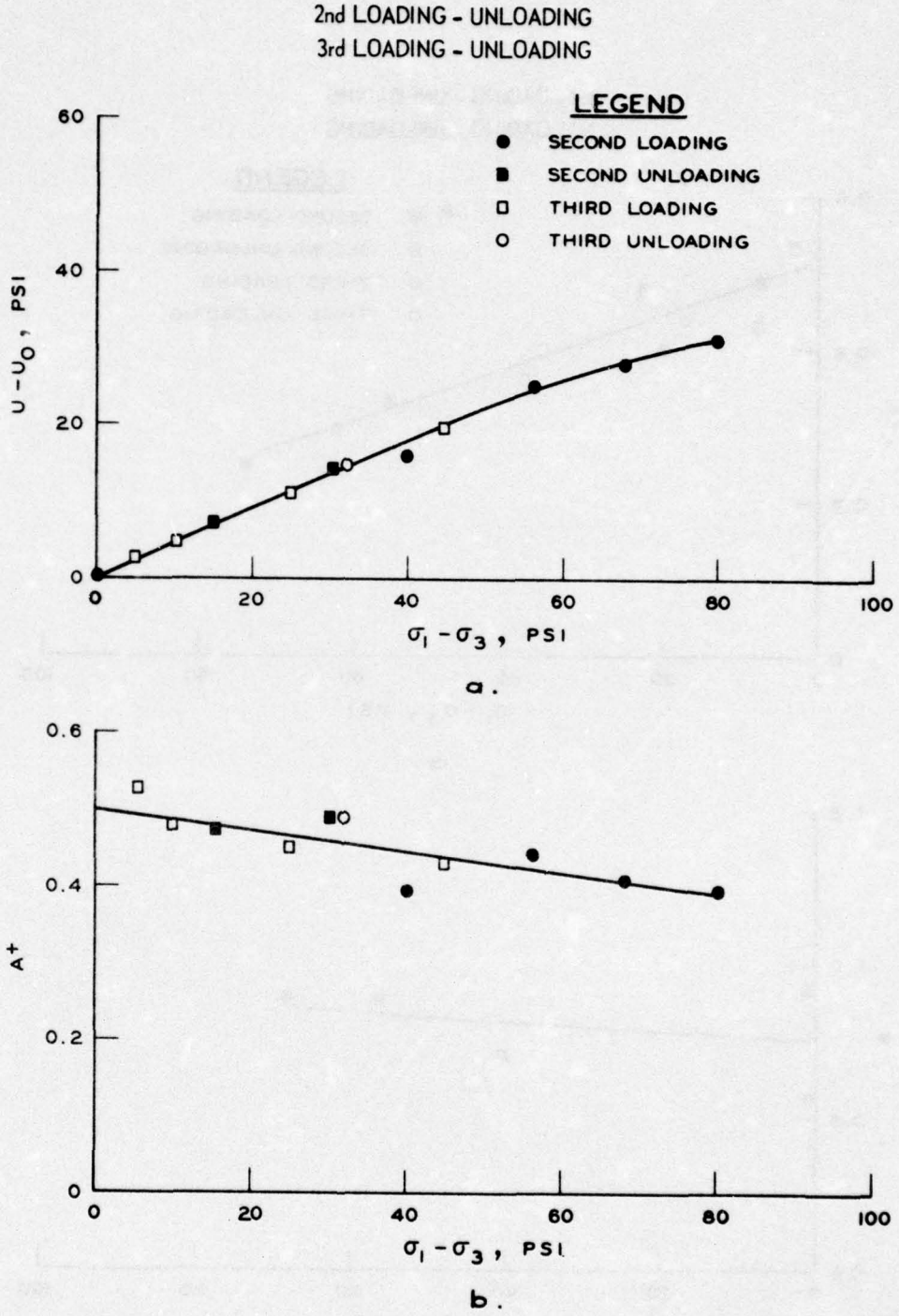
2nd LOADING - UNLOADING
3rd LOADING - UNLOADING
LEGEND
SECOND LOADING
SECOND UNLOADING
THIRD LOADING
THIRD UNLOADING
U - U0, PSI
σ1 - σ3, PSI
a.
A+
σ1 - σ3, PSI
b.

Figure 18

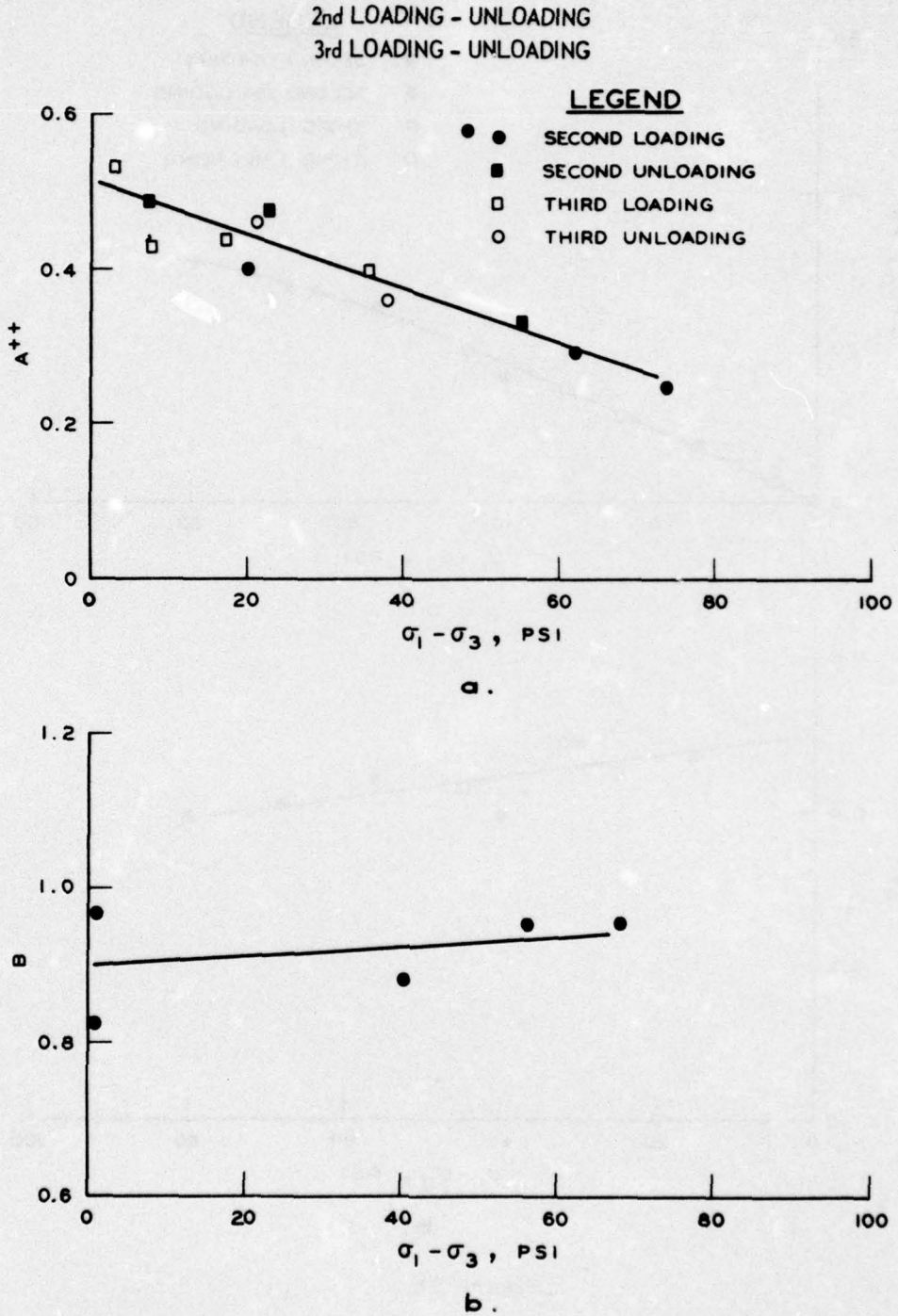
2nd LOADING - UNLOADING
3rd LOADING - UNLOADING
LEGEND
SECOND LOADING
SECOND UNLOADING
THIRD LOADING
THIRD UNLOADING
A++
0.6
0.4
0.2
0
0
20
40
60
80
100
σ1 - σ3 , PSI
a.
B
1.2
1.0
0.8
0.6
0
20
40
60
80
100
σ1 - σ3 , PSI
b.

Figure 19

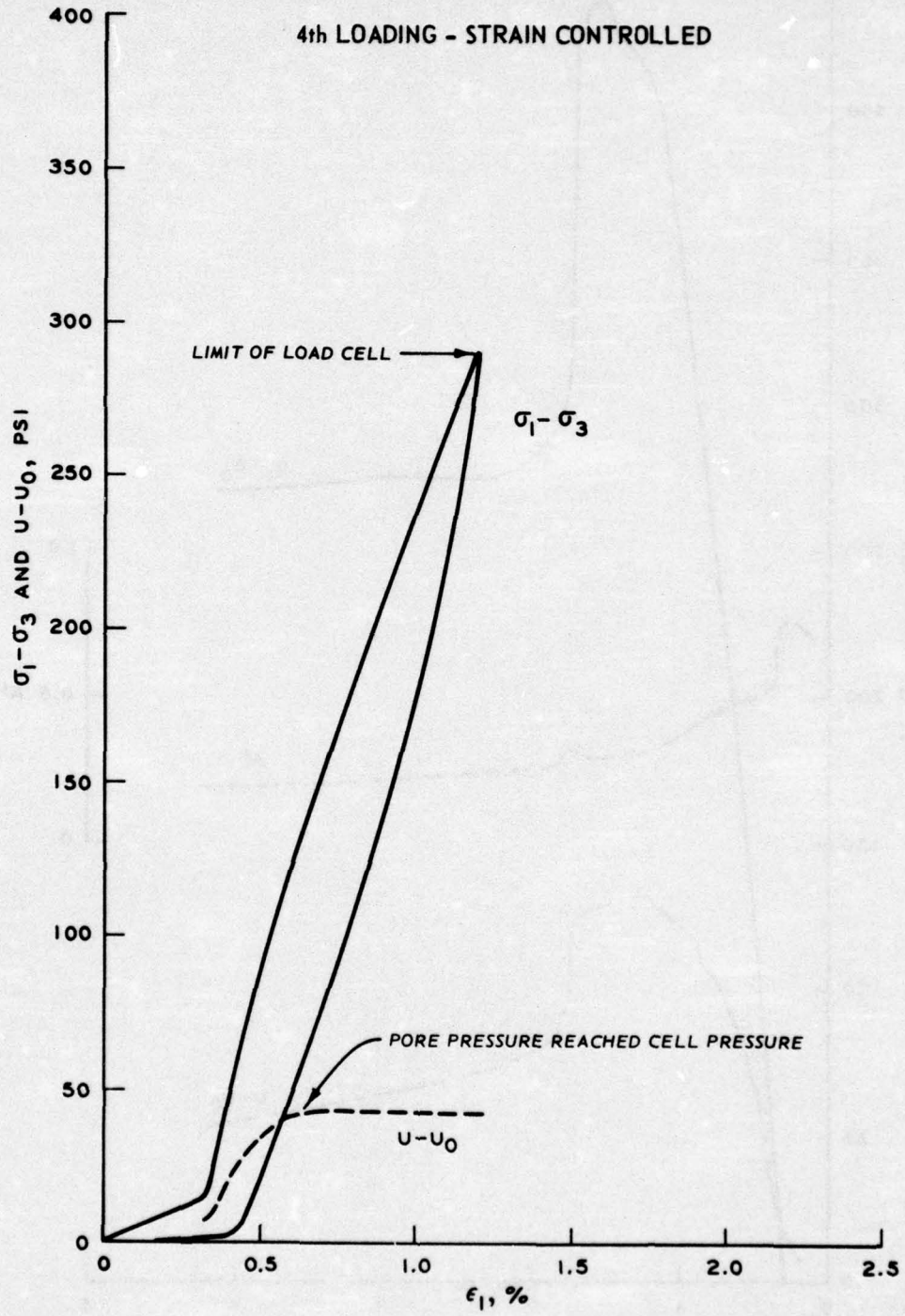
4th LOADING - STRAIN CONTROLLED
400
350
300
250
200
150
100
50
0
$\sigma_1-\sigma_3$ AND $U-U_0$, PSI
LIMIT OF LOAD CELL
$\sigma_1-\sigma_3$
PORE PRESSURE REACHED CELL PRESSURE
$U-U_0$
0
0.5
1.0
1.5
2.0
2.5
ϵ_1, %

Figure 20

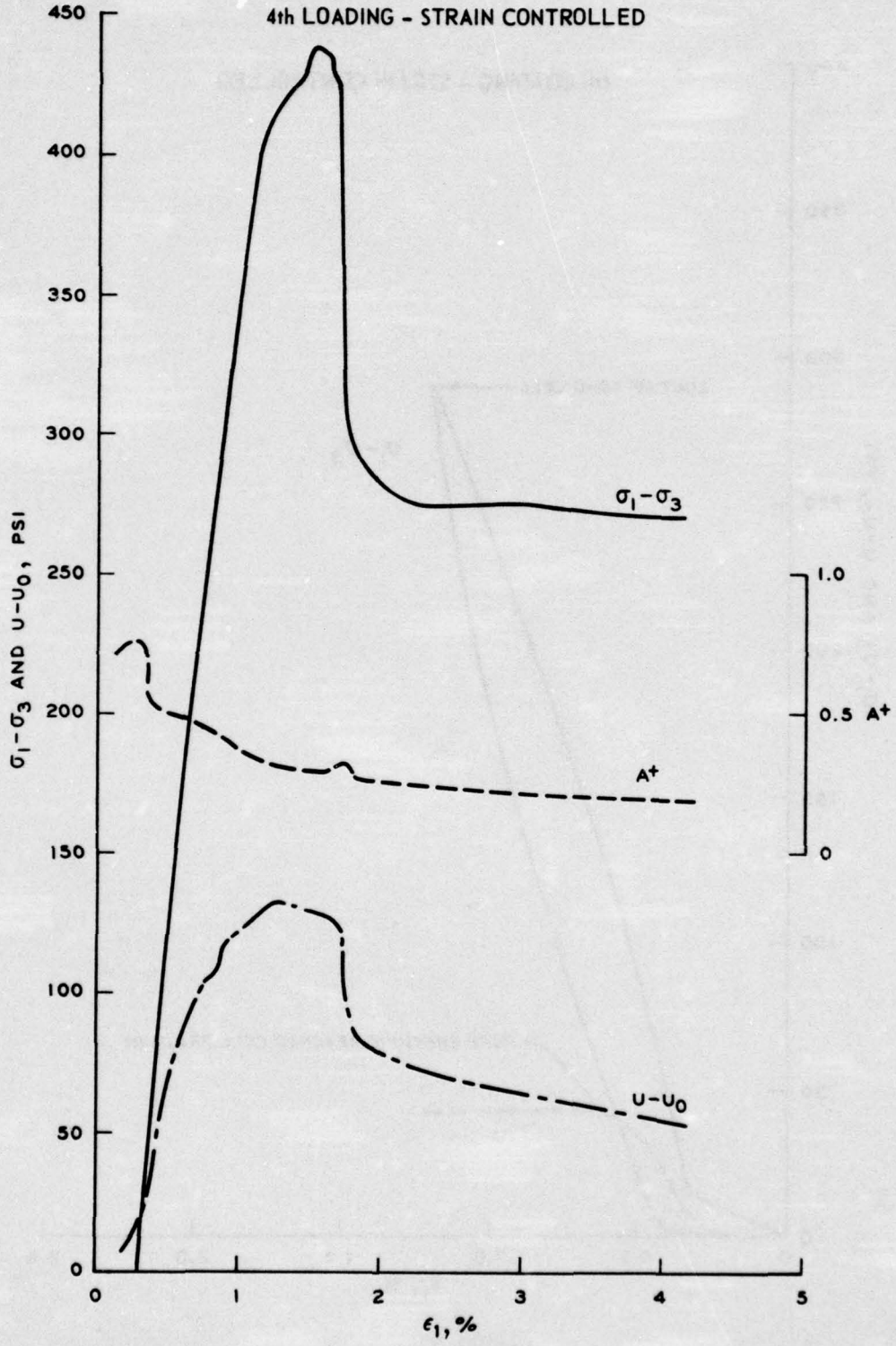
4th LOADING - STRAIN CONTROLLED
450
400
350
300
250
200
150
100
50
0
$\sigma_1-\sigma_3$ AND $U-U_0$, PSI
$\sigma_1-\sigma_3$
A^+
$U-U_0$
1.0
0.5 A^+
0
0
1
2
3
4
5
ϵ_1, %

Figure 21

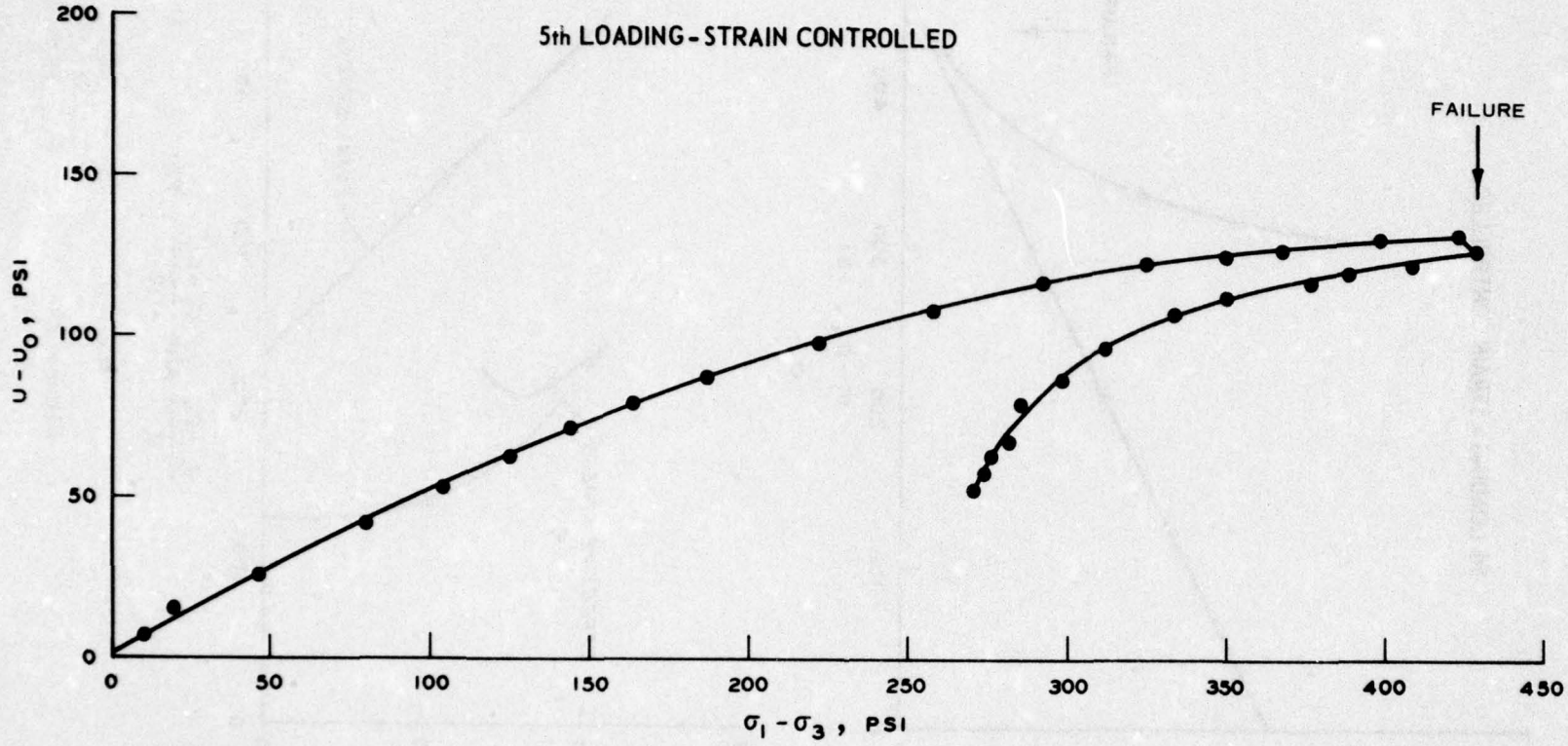
5th LOADING - STRAIN CONTROLLED
FAILURE
200
150
100
50
0
U - U0, PSI
0
50
100
150
200
250
300
350
400
450
σ1 - σ3, PSI

Figure 22

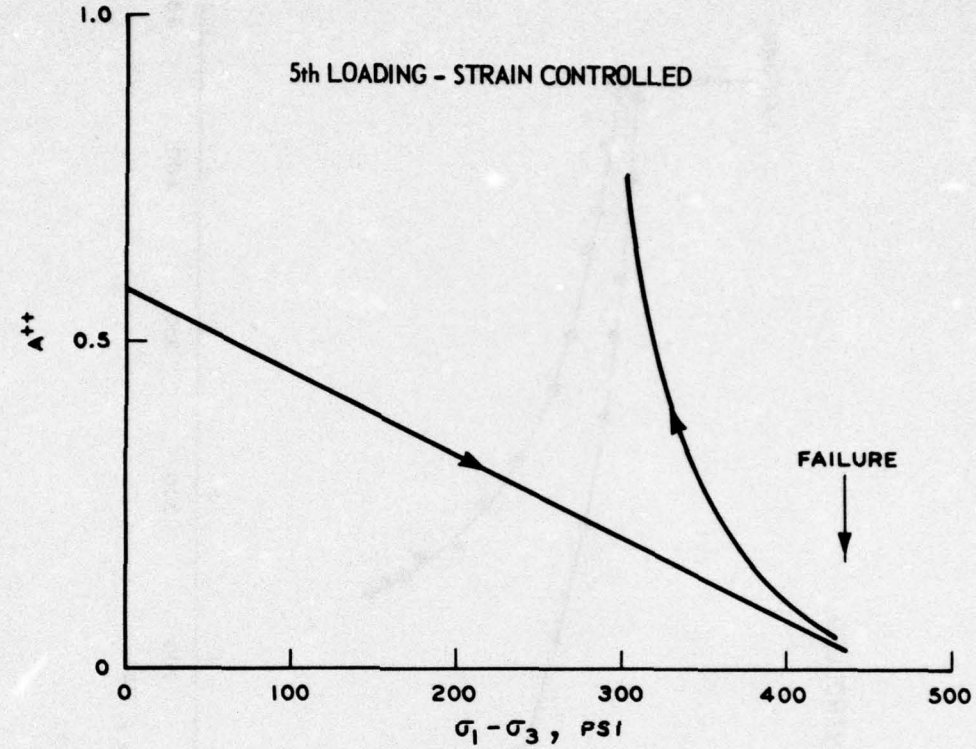
5th LOADING - STRAIN CONTROLLED
1.0
0.5
0
A^{++}
FAILURE
0
100
200
300
400
500
$\sigma_1 - \sigma_3$, PSI

a.

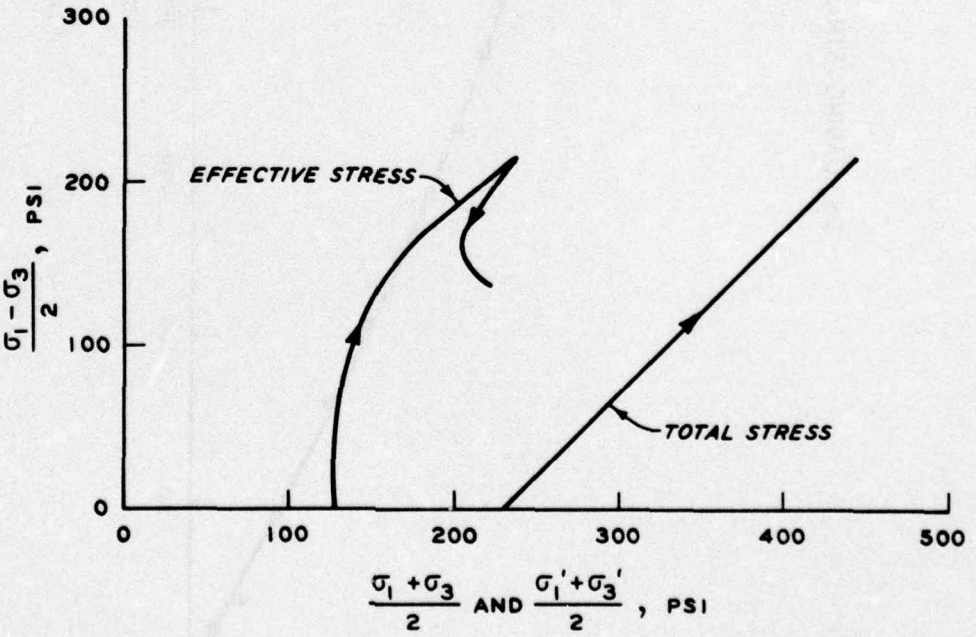
300
200
100
0
$\frac{\sigma_1 - \sigma_3}{2}$, PSI
EFFECTIVE STRESS
TOTAL STRESS
0
100
200
300
400
500
$\frac{\sigma_1 + \sigma_3}{2}$ AND $\frac{\sigma_1' + \sigma_3'}{2}$, PSI

b.

Figure 23

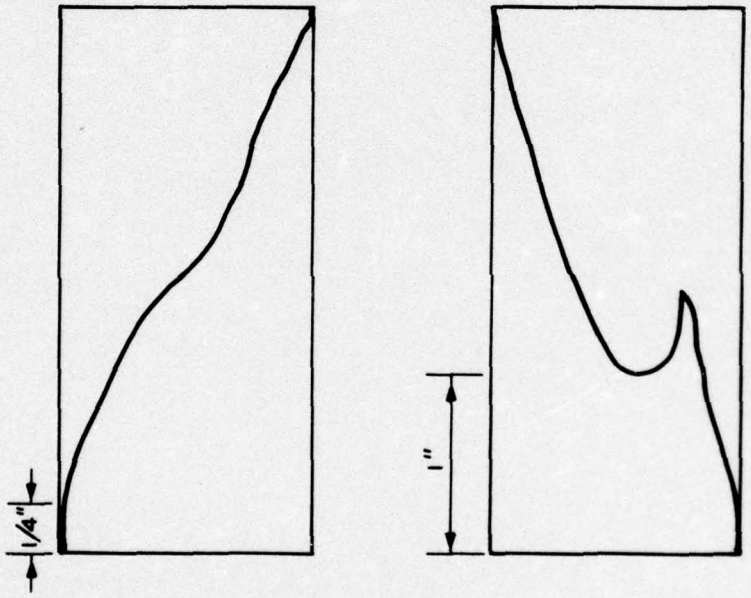

Figure 24

APPENDIX A: EFFECT OF TEMPERATURE CHANGE ON PORE PRESSURE

Effects of Temperature Rise

1. As the coefficient of thermal expansion for water is about ten times the value for the soil matrix, a rise in temperature in a sealed soil sample will cause a rise in pore pressure. The basic mechanism is an expansion of the soil water which is resisted by the soil, so that the rise in pore pressure produces a drop in effective stress leading to swelling of the soil structure. The swelling of the soil matrix plus its thermal expansion must equal the thermal expansion of the water. Thus the pore pressure developed is increased by increase in thermal expansion of water (the coefficient of thermal expansion for water is not constant, but increases with temperature as shown in Figure A1 and increases with increasing stiffness of the soil). Other factors play a minor role, but in most cases may be neglected; these include the compressibility of the water and soil grains and the influence of temperature on interparticle forces.

Experimental Evidence

2. A number of workers have published experimental evidence of pore pressure change with temperature change (e.g. Ladd,[5]* Henkel and Sowa,[2] Mitchell and Campanella,[4,6] and Plum[3]). Figure A2 shows experimental results published by Henkel and Sowa for Weald clay under cyclic temperature change. The Weald clay was consolidated to 100 psi and showed an increase of nearly 7 psi for a temperature increase of 4°C. It will be noted, too, that the effect was not reversible, residual positive pore pressures being created by the temperature cycling. Plum[3] found that the residual pore pressure became constant after about four cycles.

---

* Raised numerals refer to entries in the References listed at the end of the main text.

3. Mitchell and Campanella[4] defined an empirical parameter F where

$$F = \frac{\Delta u/\Delta t}{\sigma'} \qquad \text{(A-1)}$$

where

$\Delta u/\Delta t$ = the change in pore pressure per $1^{\circ}F$ rise in temperature

σ' = the effective stress with the same units as Δu

4. Values of Δu, σ', Δt, and F are tabulated below, taken from Plum's thesis.[3] For the clays tested, the values of F lie in the range 0.0073 to 0.013, but for a sandstone porous stone, F was found to be much higher (0.051) and this may be indicative of the order of magnitude to be expected for clay shale. There appears to be no such published information available on clay shales.

Summary of Temperature-Induced Pore Pressures (Plum[3])

Soil Type	σ' kg/cm^2	Δu kg/cm^2	Δt °F	F	Reference
Illite (grundite)	2.5	0.58	70-110	0.0073	Mitchell & Campanella[4]
San Francisco Bay mud	1.5	0.50	70-110	0.0083	Mitchell & Campanella[4]
Weald clay	7.1	0.50	77-84.2	0.0097	Henkel & Sowa[2]
Kaolinite	2.0	0.78	70-110	0.0097	Mitchell & Campanella[6]
Vicksburg clay	1.0	0.28	68-96.8	0.0097	Ladd[5]
Vicksburg clay	6.5	1.9	68-96.8	0.0101	Ladd[5]
Porous stone (sandstone)	5.8	5.2	41.5-59	0.051	Mitchell & Campanella[4]
Newfield clay	1.4	0.66	57-93	0.013	Plum[3]
Newfield clay	2.8	1.06	57-97	0.010	Plum[3]
Newfield clay	4.2	2.08	53.5-93	0.012	Plum[3]

Theoretical Behavior

5. A theoretical expression for induced pore pressures due to temperature rise can be obtained very simply by equating volume changes due to thermal expansion of water to volume change due to thermal expansion of soil matrix plus volume change of soil matrix caused by the effective stress decrease arising from the increased pore pressure (e.g. see Plum[3]). Small-order effects are ignored and the expression becomes, if the soil is fully saturated,

$$C_s \log \frac{\sigma'}{\sigma' - \Delta u} = e_o(K_w - K_s)\Delta t \qquad \text{(A-2)}$$

where

C_s = the coefficient of soil swelling, assumed to be linear on an e-log p plot

σ' = effective stress before temperature change

e_o = void ratio

K_w = coefficient of thermal volumetric expansion for water

K_s = coefficient of thermal volumetric expansion for soil

6. The value of K_w varies with temperature and it is more convenient to use $K_w \Delta t$, the change in specific volume of water (see Figure A1).

7. A further simplification can be made by putting $(K_w - K_s) = 0.9\ K_w$, since water expands about ten times as much as soil for the same temperature rise.

8. Thus, the expression developed by Plum[3] is obtained, viz:

$$\Delta u = \sigma'(1 - 10^{-B}) \qquad \text{(A-3)}$$

where

$$B = \frac{0.9 \times \Delta u_{ws} \times e_o}{C_s} \qquad \text{(A-4)}$$

where Δu_{ws} = change in specific volume of water for the temperature change considered.

9. In Equation A-2 the term $C_s \log \sigma'/(\sigma' - \Delta u)$ can be replaced by $(1 + e_o) \times \Delta u \times m_{vs}$, where m_{vs} is the coefficient of swelling, i.e. the slope of the $\Delta e/(1 + e_o)$ versus p plot. Equation A-3 then becomes:

$$\Delta u = \frac{0.9\, e_o \Delta u_{ws}}{(1 + e_o) m_{vs}} \tag{A-5}$$

Effect of Water in Pore Pressure Lines

10. The thermal expansion of equipment lines, porous stones, and pore pressure transducers is about 10 to 15 percent of that for water. Thus excess water in these elements due to temperature rise must flow into the soil, causing the soil to swell and increasing the pore pressure further. This can be allowed for theoretically by adding the water in the lines to that in the soil specimen.

11. A simple way to consider this effect is to put

$$V_{wo} + V_{wl} = RV_{wo} \tag{A-6}$$

where

V_{wo} = water volume in soil specimen

V_{wl} = water volume in ducts, etc.

Equation A-2 then becomes:

$$C_s \log \frac{\sigma'}{\sigma' - \Delta u} = e_o\, (RK_w - K_s)\Delta t$$

$$= 0.9\, Re_o K_w \Delta t \tag{A-7}$$

Equation A-3 remains the same, but B becomes:

$$B = \frac{0.9\, Re_o \Delta u_{ws}}{C_s} \tag{A-8}$$

Equation A-5 becomes:

$$\Delta u = \frac{0.9\ e_o R \Delta u_{ws}}{(1 + e_o) m_{vs}} \qquad \text{(A-9)}$$

Calculated Pore Pressure Response for Clay Shale

12. The specimen in Test T1 was allowed to swell from an effective stress of 80 psi to 20 psi and the swelling line on a $\Delta v/v_o$ versus log p plot is shown in Figure 2 at the end of the main text. It is linear on this plot. On reconsolidation, however, to 120 psi, it was not reversible and it was not linear.

13. Using the swelling line, the volume change from 80 psi to 20 psi was 0.363 percent and initial void ratio was about 0.47.

$$\frac{\Delta v}{v_o} = \frac{\Delta e}{1 + e_o}$$

$$\Delta e = 1.47 \times \frac{0.363}{100} = 0.00534$$

$$0.00534 = C_s \log \frac{80}{20}$$

$$C_s = 0.00887$$

Ignoring water in lines, etc.,

$$B = \frac{0.9 \times 0.00021 \times 0.47}{0.00887}$$

$$= 0.01001$$

$$\Delta u = \sigma' (1 - 0.977)$$

$$= 0.023\ \sigma'$$

14. Thus, the calculated response in psi is as shown on the following page:

Effective Stress σ' psi	Calculated Δu/Δt , psi/°C (1)	(2)	(3)
120	2.76	4.00	3.34
80	1.84	2.67	2.23
40	0.92	1.33	1.11
20	0.46	0.67	0.56

(1) Calculated values ignoring water in lines, etc.
(2) Calculated values taking account of water in lines.
(3) Calculated values with top pore pressure transducer closed.

15. The total volume of water in leads, porous stones, and transducers is 11 cc, of which 6 cc is in the top transducer system and 5 cc in the bottom transducer system. The volume of water in the soil specimen is about 24 cc. Thus, with both transducers operating, the value of R is

$$R = \frac{11 + 24.2}{24.2} = 1.45$$

With the bottom transducers only operating:

$$R = \frac{5 + 24.2}{24.2} = 1.21$$

Calculated values, even with the R adjustment, are markedly less than observed values.

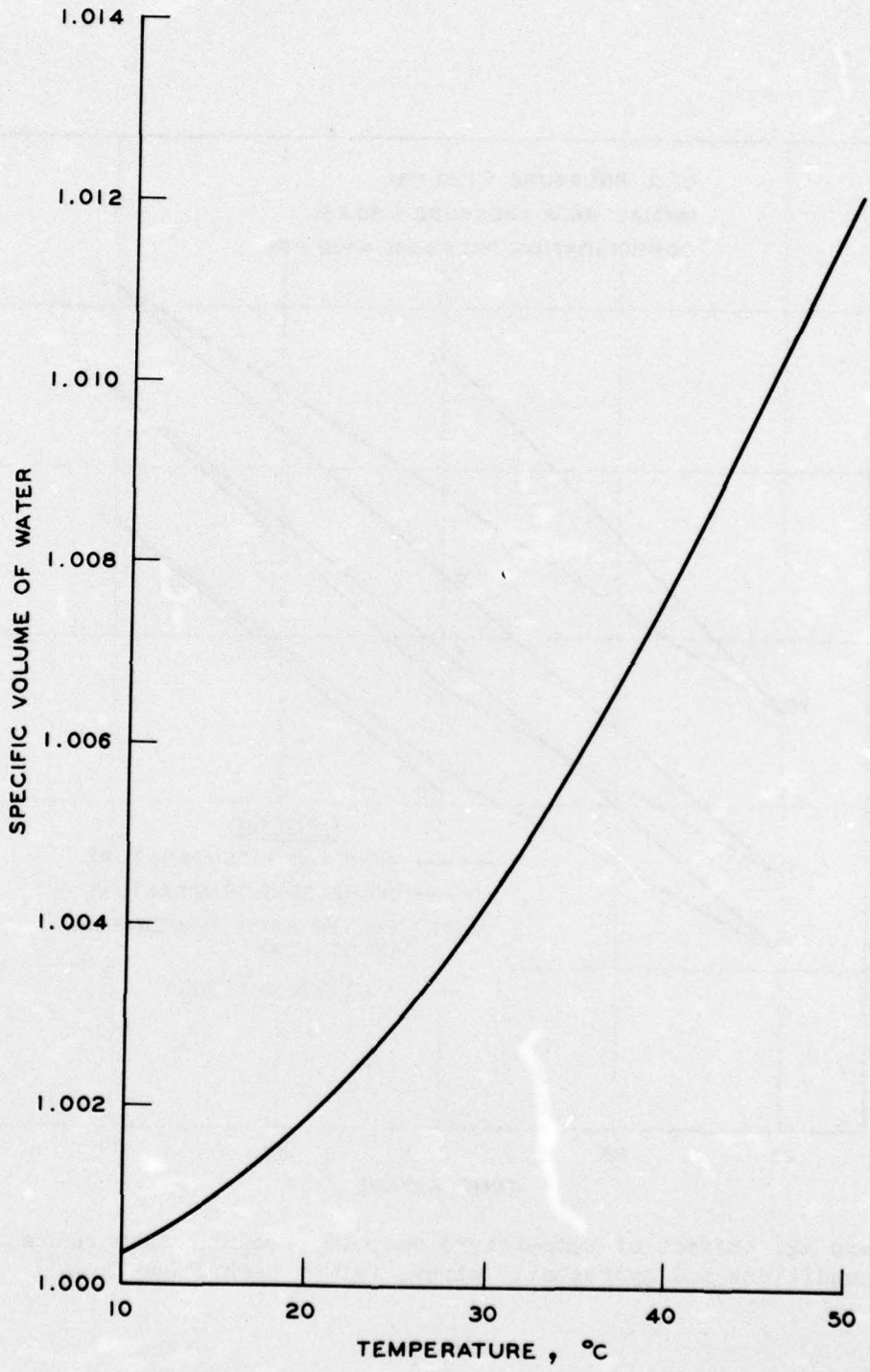

Figure A1. Specific volume of water versus temperature

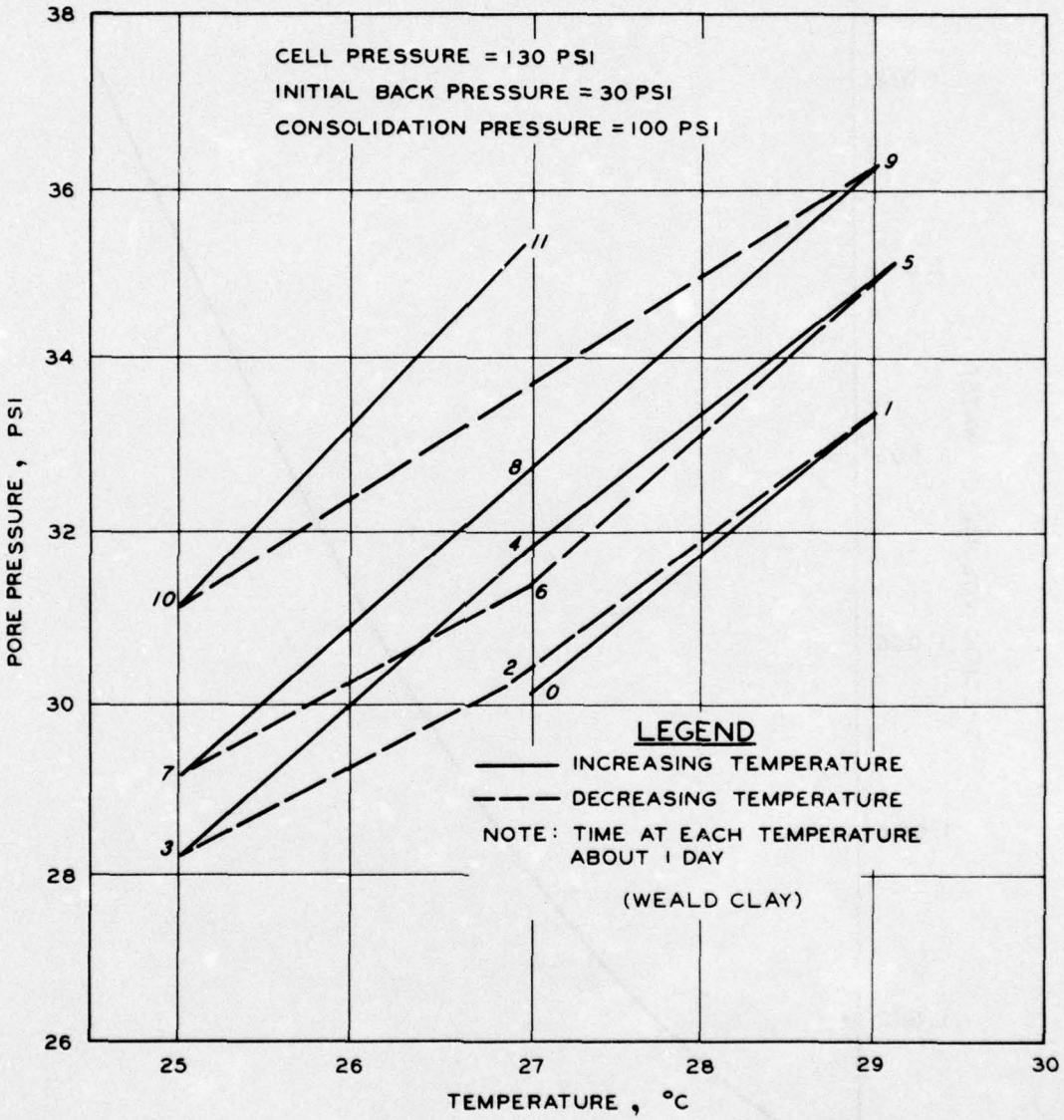

Figure A2. Effect of temperature on pore pressure under undrained conditions and hydrostatic stress (after Henkel and Sowa[2])

APPENDIX B: DEFINITION OF PORE PRESSURE PARAMETERS

1. The pore pressure parameters A and B were defined by Skempton[1*] as

$$\Delta u = B\left[\Delta\sigma_3 + A(\Delta\sigma_1 - \Delta\sigma_3)\right] \tag{B-1a}$$

$$= B\Delta\sigma_3 + BA(\Delta\sigma_1 - \Delta\sigma_3) \tag{B-1b}$$

In most saturated soils B = 1.0 and Equation B-1 reduces to

$$\Delta u = \Delta\sigma_3 + A(\Delta\sigma_1 - \Delta\sigma_3) \tag{B-2}$$

2. In saturated clay shale, however, the value of B is less than 1.0 as the stiffness of the soil structure is significant in relation to that of water. Measured values of B for the Taylor clay shale of this study ranged from 0.82 to 0.96.

3. The portion of pore pressure change due to change in deviator stress given in Equation B-1b is

$$\Delta u = BA(\Delta\sigma_1 - \Delta\sigma_3) \tag{B-3}$$

4. However, Δu can be measured either from the first application of deviator stress or over any incremental change of deviator stress. Consequently, two parameters are defined here, A^+ and A^{++}, where

$$A^+ = BA \tag{B-4}$$

$$\Delta u = A^+(\Delta\sigma_1 - \Delta\sigma_3) \tag{B-5}$$

---

* Raised numerals refer to entries in the References listed at the end of the main text.

for the change in pore pressure and deviator stress from the start of shearing and

$$A^{++} = BA$$

$$\Delta u = A^{++} (\Delta\sigma_1 - \Delta\sigma_3)$$

for any incremental change in pore pressure for an incremental change in deviator stress during shearing.

5. Thus, as shown in Figure B1, A^{+} is a secant value of BA in a plot of $(u - u_o)$ versus $(\sigma_1 - \sigma_3)$ whereas A^{++} is the slope of the curve at any point (or alternately the secant value over an increment of the curve).

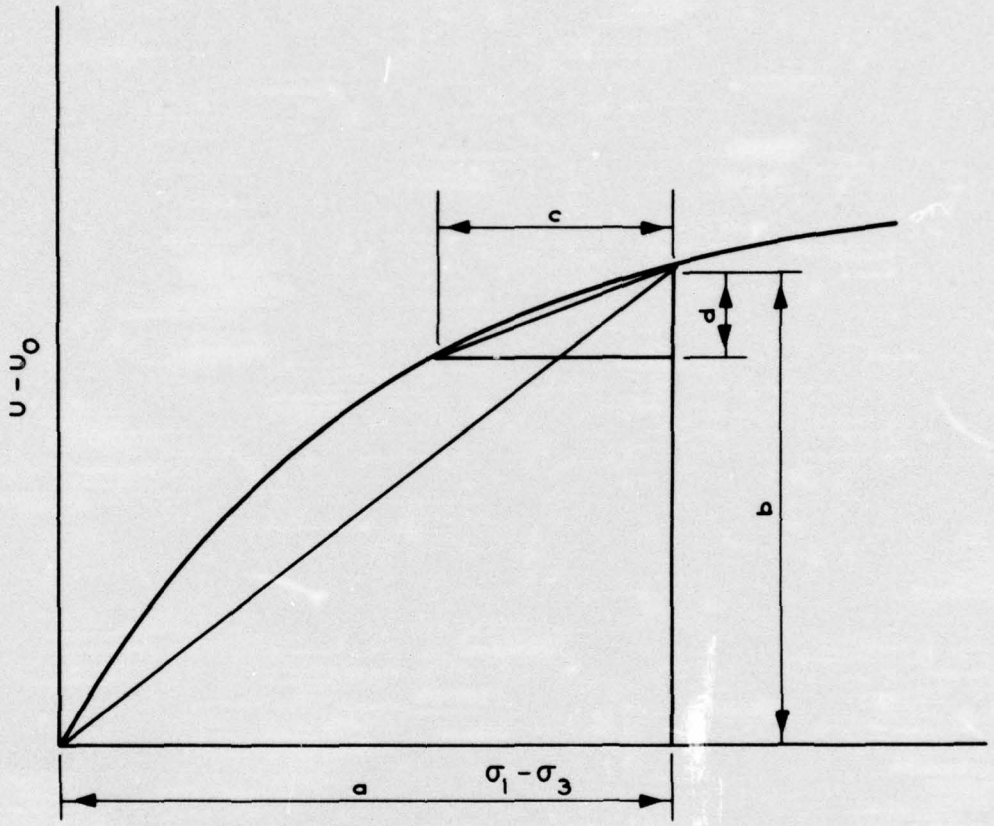

$$A^{+} = b/a$$
$$A^{++} = d/c$$

Figure B1. Definition of pore pressure parameters

APPENDIX C: INFLUENCE OF ANISOTROPY ON PORE PRESSURE

(References: Atkinson,[7*] Gibson,[8] Harr,[9] Henkel,[10] Pickering[11])

1. Consider a saturated triaxial test specimen in which:

E_1' = vertical effective stress Young's modulus

E_3' = transverse effective stress Young's modulus

ν_1' = Poisson's ratio with respect to effect of transverse strains on transverse strains

ν_2' = Poisson's ratio with respect to effect of vertical strains on transverse strains

ν_3' = Poisson's ratio with respect to effect of transverse strains on vertical strains

$$\text{Note: } \frac{\nu_2'}{E_1'} = \frac{\nu_3'}{E_3'} \text{ for elastic energy} \tag{C-1}$$

2. Submit this specimen to undrained triaxial deformation in which the changes in vertical and horizontal effective stresses are $\Delta\sigma_1'$ and $\Delta\sigma_3'$, respectively (note: $\Delta\sigma_2' = \Delta\sigma_3'$). Then volume change ε_v is given by

$$\varepsilon_v = \varepsilon_1 + 2\varepsilon_3 \tag{C-2}$$

$$\varepsilon_1 = \frac{1}{E_1'}(\Delta\sigma_1' - 2\nu_2'\Delta\sigma_3') \tag{C-3a}$$

$$\varepsilon_3 = \frac{\Delta\sigma_3'}{E_3'}(1 - \nu_1') - \frac{\nu_2'\Delta\sigma_1'}{E_1'} \tag{C-3b}$$

Putting $E_3'/E_1' = n'$

---

* Raised numerals refer to entries in the References listed at the end of the main text.

$$\varepsilon_v = \frac{1}{E'_1}\left[(\Delta\sigma'_1 - 2\nu_2\Delta\sigma'_3 - 2\nu_2\Delta\sigma'_1) + \frac{2\Delta\sigma'_3}{n'}(1 - \nu'_1)\right] \qquad \text{(C-4)}$$

or

$$\varepsilon_v = \frac{1}{E'_1}\left[(\Delta\sigma_1 - \Delta u) - 2\nu'_2(\Delta\sigma_3 - \Delta u) - 2\nu'_2(\Delta\sigma_1 - \Delta u) + \frac{2(1 - \nu'_1)}{n'}(\Delta\sigma_3 - \Delta u)\right] \qquad \text{(C-5)}$$

3. But the volume change in the rock structure must equal the volume change in the pore fluid (e.g. see Skempton[1]). If K_w is the bulk modulus for the pore fluid and m is the porosity, then the volume change ε_v in the pore fluid contained in unit volume of rock is:

$$\varepsilon_v = \frac{\Delta u \times m}{K_w} \qquad \text{(C-6)}$$

Equating Equations C-5 and C-6 gives:

$$\frac{\Delta u \times m \times E'_1}{K_w} = \left\{\Delta\sigma_1(1 - 2\nu'_2) + \Delta\sigma_3\left[\frac{2(1 - \nu'_1)}{n'} - 2\nu'_2\right] - \Delta u\left[1 - 4\nu'_2 + \frac{2(1 - \nu'_1)}{n'}\right]\right\} \qquad \text{(C-7)}$$

from which:

$$\Delta u = \frac{\Delta\sigma_1(1 - 2\nu'_2) + 2\Delta\sigma_3\left(\frac{1 - \nu'_1}{n'} - \nu'_2\right)}{\frac{mE'_1}{K_w} + \left[1 - 4\nu'_2 + \frac{2(1 - \nu'_1)}{n'}\right]} \qquad \text{(C-8)}$$

Putting

$$Y = 1 - 4\nu'_2 + \frac{2(1 - \nu'_1)}{n'} \qquad \text{(C-9)}$$

then Equation C-8 can be written in the form:

$$\Delta u = \frac{Y}{\frac{mE'_1}{K_w} + Y}\left[\Delta\sigma_3 + \frac{1 - 2\nu'_2}{Y}(\Delta\sigma_1 - \Delta\sigma_3)\right] \qquad \text{(C-10)}$$

By definition (Skempton[1]):

$$\Delta u = B\left[\Delta\sigma_3 + A(\Delta\sigma_1 - \Delta\sigma_3)\right] \qquad \text{(C-11)}$$

Thus, from Equations C-10 and C-11

$$B = \frac{Y}{\frac{mE'_1}{K_w} + Y}$$

$$= \frac{1 - 4\nu'_2 + \frac{2(1 - \nu'_1)}{n'}}{\frac{mE'_1}{K_w} + \left[1 - 4\nu'_2 + \frac{2(1 - \nu'_1)}{n'}\right]} \qquad \text{(C-12)}$$

and

$$A = \frac{1 - 2\nu'_2}{Y}$$

$$= \frac{1 - 2\nu'_2}{1 - 4\nu'_2 + \frac{2(1 - \nu'_1)}{n'}} \qquad \text{(C-13)}$$

The value of A is thus independent of the compressibility of the rock-pore fluid system, which Skempton[1] showed for the isotropic elastic case.

4. Typical values of A from Equation C-13 are given below and plotted in Figure C1 for n' values ranging from 1.0 to 5.0 and ν'_1 values of 0.1 and 0.2. The value of ν'_2 has been assumed to be related to ν'_1 by the expression suggested by Henkel,[10] viz:

$$\nu'_1 = \frac{\nu'_2 + \nu'_3}{2} \qquad \text{(C-14)}$$

or, combining Equations C-1 and C-14,

$$\nu_1' = \nu_2' \left(\frac{1 + n'}{2} \right)$$

	Calculated A Values	
n'	$\nu_1' = 0.1$	$\nu_1' = 0.2$
1.0	0.33	0.33
1.25	0.39	0.41
1.5	0.45	0.48
1.75	0.49	0.53
2.0	0.53	0.58
3.0	0.64	0.71
5.0	0.76	0.82
	1.0	1.0

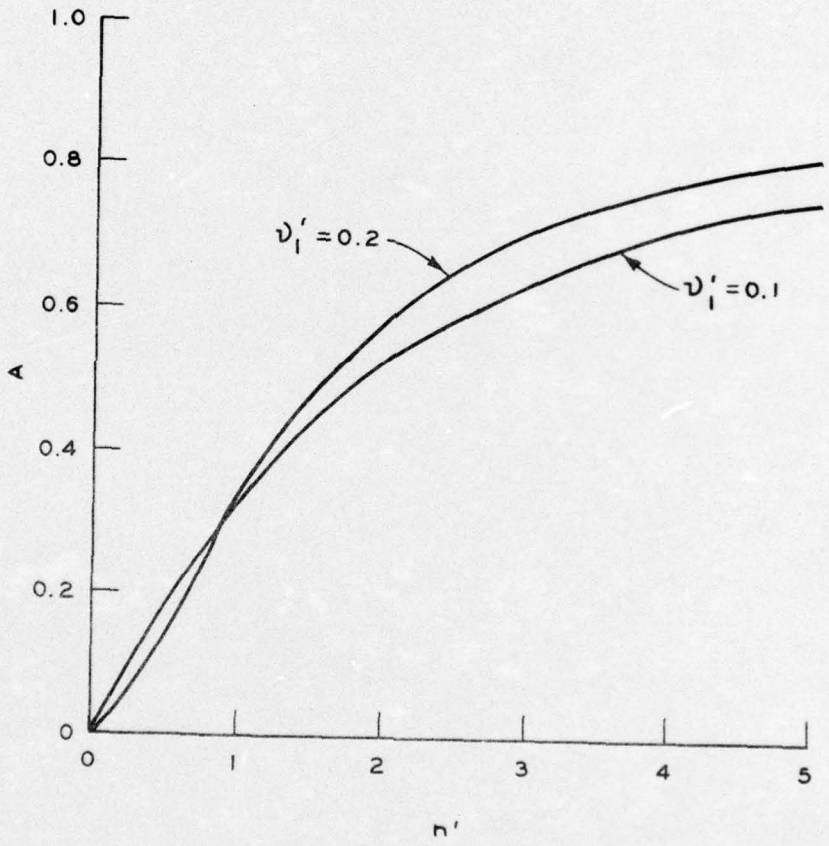

Figure C1

In accordance with ER 70-2-3, paragraph 6c(1)(b), dated 15 February 1973, a facsimile catalog card in Library of Congress format is reproduced below.

Parry, R H G
Engineering properties of clay shales; Report 3: Preliminary triaxial test program on Taylor shale from Laneport Dam, by R. H. G. Parry. Vicksburg, U. S. Army Engineer Waterways Experiment Station, 1976.
1 v. (various pagings) illus. 27 cm. (U. S. Waterways Experiment Station. Technical report S-71-6, Report 3)
Prepared for Office, Chief of Engineers, U. S. Army, Washington, D. C.
Includes bibliography.

1. Clay shales. 2. Laneport Dam. 3. Taylor shale. 4. Shales. 5. Triaxial shear tests. I. U. S. Army. Corps of Engineers. (Series: U. S. Waterways Experiment Station. Technical report S-71-6, Report 3)
TA7.W34 no.S-71-6 Report 3


FILM